Research Article

Ghfren S. Aloraini, Mona Othman I. Albureikan, Aisha M. A. Shahlol, Taghreed Shamrani, Hussam Daghistani, Mohammad El-Nablaway, Nagwa A. Tharwat, Ahmed M. Elazzazy, Ahmed F. Basyony, and Ahmed Ghareeb*

Biomedical and therapeutic potential of marine-derived *Pseudomonas* sp. strain AHG22 exopolysaccharide: A novel bioactive microbial metabolite

https://doi.org/10.1515/rams-2024-0016
received November 16, 2023; accepted April 03, 2024

Abstract: Microbial exopolysaccharides (EPSs) are gaining interest as alternatives to chemical antioxidants and pharmaceuticals. This study mines the promising biomedical and antimicrobial potential of a marine bacterium, a prolific EPS producer, isolated from the Red Sea. *Pseudomonas* sp. strain AHG22 generated an EPS weighing 6.98 g·L^{-1}, coded EPSF8, subjected to FT-IR and HPLC chemical analysis. EPSF8 was then investigated for antioxidant assessment by 2,2-diphenyl-1-picrylhydrazyl (DPPH), H_2O_2, ABTS$^{\cdot+}$, nitric oxide, total antioxidant capacity (TAC), and ferric reducing antioxidant power (FRAP). EPSF8 had an IC_{50} of 46.99 μg·mL^{-1} in the DPPH antioxidant assay and antioxidant capacities of 219.45 μg·mg^{-1} ascorbic acid equivalent (AAE) in the TAC assay and 54.15 μg·mg^{-1} AAE in the FRAP assay. The *in vitro* anti-inflammatory effect of EPSF8 was tested against 5-lipoxygenase (5-LOX) and cyclooxygenase-2 (COX-2) enzymes and compared with the drugs ibuprofen and celecoxib used as controls. The IC_{50} values of 5-LOX, COX-2, ibuprofen, and celecoxib were found to be 14.82, 15.49, 1.5, and 0.28 μg·mL^{-1}, respectively. Additionally, EPSF8 revealed antidiabetic activity toward α-amylase and α-glucosidase, and the IC_{50} values were 93.1 and 127.28 μg·mL^{-1}, compared to those of acarbose (50.93 and 4.13 μg·mL^{-1}, respectively). Anti-obesity activity of EPSF8 by lipase inhibition revealed IC_{50} = 56.12 μg·mL^{-1} compared to orlistat (IC_{50} = 20.08 μg·mL^{-1}) as a control. EPSF8 displayed antibiofilm and bactericidal activity against Gram-positive (G +ve) and Gram-negative (G −ve) ATCC pathogenic bacterial strains. It had a minimum bactericidal concentration/minimum inhibitory concentration ratio ≤2, indicating a broad bactericidal spectrum. Furthermore, EPSF8 is evidenced to have a promising anti-butyrylcholinesterase activity for the control of Alzheimer's disease. The findings of the present analysis suggest that the isolated *Pseudomonas* sp. strain AHG22 EPS can potentially be explored as a promising green therapeutic compound.

Keywords: antioxidant, anti-inflammatory, antidiabetic, anti-obesity, antibiofilm, anti-Alzheimer

*** Corresponding author: Ahmed Ghareeb**, Botany and Microbiology Department, Faculty of Science, Suez Canal University, Ismailia 41522, Egypt, e-mail: aghareeb@science.suez.edu.eg
Ghfren S. Aloraini: Department of Medical Laboratory, College of Applied Medical Sciences, Prince Sattam Bin Abdulaziz University, Al-Kharj 11942, Saudi Arabia, e-mail: g.aloraini@psau.edu.sa
Mona Othman I. Albureikan: Department of Biological Sciences, Faculty of Science, King Abdulaziz University, Jeddah 21589, Saudi Arabia, e-mail: malboraikan@kau.edu.sa
Aisha M. A. Shahlol: Department of Medical Laboratory Technology, Faculty of Medical Technology, Wadi-Al-Shatii University, Brack, Libya, e-mail: As.shahlol@wau.edu.ly
Taghreed Shamrani: Department of Clinical Biochemistry, Faculty of Medicine, King Abdulaziz University, Jeddah 21589, Saudi Arabia; Food, Nutrition and Lifestyle Unit, King Fahd Medical Research Centre, King Abdulaziz University, Jeddah 21551, Saudi Arabia, e-mail: tshumrani@kau.edu.sa
Hussam Daghistani: Department of Clinical Biochemistry, Faculty of Medicine, King Abdulaziz University, Jeddah 21589, Saudi Arabia; Regenerative Medicine Unit, King Fahd Medical Research Center, King Abdulaziz University, Jeddah 21589, Saudi Arabia, e-mail: hmdaghistani@kau.edu.sa
Mohammad El-Nablaway: Department of Medical Biochemistry, Faculty of Medicine, Mansoura University, Mansoura 35516, Egypt; Department of Basic Medical Sciences, College of Medicine, AlMaarefa University, Diriyah, 13713, Riyadh, Saudi Arabia, e-mail: mnablawi@um.edu.sa, medo_bio@mans.edu.eg
Nagwa A. Tharwat: Department of Botany and Microbiology, Faculty of Science, Cairo University, Giza 12613, Egypt, e-mail: nagwa@sci.cu.edu.eg
Ahmed M. Elazzazy: Department of Biological Sciences, College of Science, University of Jeddah, Jeddah 23218, Saudi Arabia; Chemistry of Natural and Microbial Products Department, Pharmaceutical and Drug Industries Research Institute, National Research Centre, Dokki, Giza 12622, Egypt, e-mail: amelazzazy@uj.edu.sa
Ahmed F. Basyony: Microbiology and Immunology Department, Faculty of Pharmacy, Egyptian Russian University 11829, Cairo, Egypt, e-mail: ahmed-faroukbasyony@eru.edu.eg

1 Introduction

In recent years, there has been growing scholarly interest in meticulously examining and discerning microorganisms and their exopolysaccharides (EPSs) as plausible and invaluable biomedical products [1]. Utilizing microbial EPSs in the pharmaceutical sector presents a promising avenue for exploration, offering a viable alternative to chemical antioxidants. This alternative is particularly appealing due to the adverse long-term effects and safety concerns associated with conventional chemical antioxidants [2].

Several studies have demonstrated the ability of specific polysaccharides to enhance cellular defense mechanisms while concurrently mitigating the deleterious effects induced by reactive oxygen species (ROS) [3]. These polysaccharides have been found to impede the accumulation of free radicals, thereby preventing lipid peroxidation [4]. Expanded polysaccharides (EPSs) are strategically utilized as efficacious radical scavengers to safeguard the body from the deleterious effects of free radicals, which have been implicated in the etiology of diverse chronic health conditions [5]. Presently, there are recent reports of the antioxidant capacities of EPS, including those of marine origin, *Bacillus subtilis* [6], *Bacillus cereus* [7], *Kocuria* sp. [8] and *Bacillus velezensis* [9] and *Bacillus licheniformis* [10].

Marine microorganisms have also been reported to generate immunomodulatory extracellular polysaccharides (EPSs). These EPSs have been shown to influence the immune response in various ways [11]. For instance, an EPS known as EPS2E1 was isolated from the marine bacterium *Halomonas* sp. and showed intense immune-enhancing action by primarily stimulating the mitogen-activated protein kinase and nuclear factor kappa-light-chain-enhancer of activated B cells (NF-κB) pathways [12]. Sphingobactan, an alpha-mannan EPS extracted from *Arctic Sphingobacterium* sp., considerably dwindled the amount of nitric oxide (NO) produced by LPS-activated macrophages [13]. Chatterjee *et al.* hypothesized that sphingobactan might activate macrophages' *in vitro* anti-inflammatory activities.

The significance of EPS in tackling infectious diseases has been recently investigated. Extensive reports have demonstrated that marine microbial EPS possesses remarkable immune-modulating and antiviral properties, exhibiting promising potential in inhibiting specific strains of influenza viruses and bacteria. A marine polysaccharide was explored by Abdalla *et al.* to have strong antibacterial properties and effectively inhibit uropathogenic *Escherichia coli* (UPEC) [14,15]. This could be an alternative, antibiotic-free treatment for urinary tract infections [16]. Similarly, Wu *et al.* found that an EPS (EPS273) synthesized *P. stutzeri* 273 had an anti-biofilm effect and could inhibit *Pseudomonas aeruginosa* [17].

Carbohydrate metabolism involves two primary glycosidases: α-glucosidase and α-amylase. The inhibitors of these enzymes are used in the treatment of, notably, type 2 diabetes and obesity [18,19]. Microbes generate desirable glycosidase-inhibiting compounds. These compounds have immense potential as pharmaceuticals and dietary supplements. *Actinoplanes* sp.'s acarbose, an inhibitor of glucosidase, is highly effective in treating type 2 diabetes [20]. This marketed medication class, though adequate for treating type 2 diabetes, has significant limitations as a medication. It can cause side effects like abdominal discomfort, diarrhea, and flatulence and has restrictions, including high costs and low patient compliance. This indicates the demand for innovative classes of glucosidases derived from microorganisms with greater compliance, socioeconomic benefits, and safety prospects [21].

While microbial EPS has shown promise as an alternative to synthetic antioxidants and antibiotics, the biomedical potential of *Pseudomonas* EPS is relatively underexplored. We hypothesize that marine *Pseudomonas* sp. strain AHG22's EPS exhibits significant bioactivity supporting pharmaceutical applications. The present investigation comprehensively represents the isolation and identification process of *Pseudomonas* sp. strain AHG22 obtained from the Red Sea, employing morphological, biochemical, and 16S rRNA techniques. In addition to producing EPS, this study also examines its chemical composition and analysis. Finally, it sheds light on the extensive *in vitro* pharmacological profiling of the metabolite, including antioxidant, anti-inflammatory, anti-Alzheimer, metabolic, antimicrobial, and antibiofilm assays.

2 Materials and methods

2.1 Isolation and sampling of bacteria from the Red Sea

A 500 mL seawater sample was collected from the western coastline of the Red Sea, Saudi Arabia, in March 2023. The sample was gathered from the sea surface using a sterile container and transported to the lab in an insulated container at 4°C. In the lab, serial dilution and marine media were made by adding the following ingredients: glucose (20 g), $CaCO_3$ (1.0 g), NH_4NO_3 (0.8 g), KH_2PO_4 (0.05 g), K_2HPO_4 (0.6 g), $MgSO_4{\cdot}7H_2O$ (0.05 g), $MnSO_4{\cdot}4H_2O$ (0.1 g), and yeast extract (0.1 g) were mixed in750 mL of seawater to produce 1 L [22].

2.1.1 Selection and identification of bacterial strains

Bacterial strains were selected based on their culture growth [23] and their maximum (EPSs) synthesis rate. A 16S rRNA sequence was performed for genetic classification, and phylogenetic analysis was conducted: The forward primer was 5′-TCCGTAGGTGAACTTTGCGG 3′, and the reverse primer was 5′-TCCTCCGCTTATTGATATGC-3′ [24]. The gained DNA sequence was compared to the GenBank database at the NCBI using the BLAST tool. An alignment was then performed to determine how closely the sequence of the isolate resembled those in the database.

2.2 Production and fractional precipitation of the EPS

The promising strain F8 was chosen for EPS production based on culture, physiology, and biochemical characteristics. The bacterial isolate F8 was cultured in a broth containing yeast extract (2 g·L^{-1}), sucrose (20 g·L^{-1}), and peptone (4 g·L^{-1}). These constituents were put into 750 mL of seawater and then made up to 1 L. After growing, the bacteria were separated by spinning at 4,000 rpm at 4°C for 30 min. TCA (10%) was incorporated to eliminate protein, and the mixture was placed at 4°C and left overnight. The solution was spun again for 20 min at 5,000 rpm, and the liquid on top was kept separate. The pH of the liquid supernatant was then adjusted to 7 using NaOH solution. After that, the supernatant was precipitated with cold C_2H_5OH and centrifuged. The residue was re-dissolved, dialyzed for 72 h, and fractionally precipitated with four successive increasing volumes of C_2H_5OH [25]. Then, the UV absorption spectra within the wavelength range of 200–800 nm were analyzed to ascertain the presence of proteins and nucleic acids [26].

2.3 Characterization of EPS using FT-IR, colorimetric, and HPLC techniques

FTIR spectra were examined by mixing 2.0 mg of EPS with 200 mg of KBr pellets, and the mixture was subjected to FTIR spectroscopy using a Bruker Vector 22 Spectrophotometer [27]. Uronic acid was detected in the sample using the colorimetric technique elucidated by Filisetti-Cozzi and Carpita, in which EPS was diluted with 2 mL of concentrated H_2SO_4, boiled at 100°C for 20 min, cooled, and then 150 mL of m-hydroxy diphenyl was added, and the absorbance of the mixture was measured at 520 nm after 60 min [28]. The sulfate content was quantified using Garrido's method, in which 5 mg of EPS was hydrolyzed with 5 mL of 88% formic acid at 105°C for 5 h. After drying, 10 mg of $BaCl_2$ was dissolved in a small amount of H_2O, Tween 20 (20 mL) was supplemented, and the total volume was brought up to 100 mL in a flask. To a 10 mL hydrolysate, 1 mL of 0.3 N HCl and 1 mL of the $BaCl_2$-Tween 20 reagent were added. After mixing and standing for 15 min, the optical density was read at 500 nm [29].

The technique outlined by Randall *et al.* [30] was applied to explore the monosaccharide composition. EPS was first hydrolyzed with 2 M CF_3COOH at 120°C for 120 min. The resulting solution was subjected to dilution in CH_3OH and subsequent vacuum drying. The ensuing residue was solubilized in H_2O and examined using an Aminex carbohydrate HP-87C column (300 × 7.8 mm) with a flow rate of 0.5 mL·min^{-1}, and H_2O was the eluent.

The UV absorption spectra within the wavelength range of 200–800 nm were analyzed to detect proteins and nucleic acids [26].

2.4 Antioxidant evaluation of the EPS

2.4.1 DPPH assay

The antioxidant activity of the EPS was examined at different concentrations (1.9, 3.9, 7.8, 15.6, 31.2, 62.5, 125, 250, 500, and 1,000 μg·mL^{-1}) using the method outlined by Brand-Williams *et al.* [31], where 0.1 mM solution of 1,1-diphenyl-2-picryl hydrazyl (DPPH) in C_2H_5OH was prepared. Then, 1 mL of this solution was added to 3 mL of the EPS sample in C_2H_5OH at different concentrations (1.9–1,000 μg·mL^{-1}). The mixture was shaken and left at room temperature for 30 min. Absorbance was detected at 517 nm using a spectrophotometer (UV-VIS milton roy). The reference standard used in the experiment was ascorbic acid, and the testing process was conducted in triplicate:

$$\text{DPPH scavenging inhibition (\%)} = (\text{Ab}_{517\text{ of control}} - \text{Ab}_{517\text{ of sample}}/\text{Ab}_{517\text{ of control}}) \times 100.$$

2.4.2 H_2O_2 assay

The ability of the EPS to remove H_2O_2 was assessed, according to Ruch *et al.* EPS was prepared at different concentrations (100, 300, 500, and 1,000 μg·mL^{-1}) in 0.1 M phosphate buffer (pH = 7.4). EPS solutions were incubated with 43 mM H_2O_2 in phosphate buffer in the dark at room temperature. The absorption at 230 nm was measured during 15–60 min to assess changes over time [32]:

$$H_2O_2 \text{ scavenging } (\%) = (Ab_{230 \text{ of control}} - Ab_{230 \text{ of sample}}/Ab_{230 \text{ of control}}) \times 100.$$

2.4.3 ABTS$^{\cdot+}$ assay

The extracted EPS was assessed at different concentrations (100–1,000 μg·mL^{-1}) following the methodology described by Miller and Rice-Evans. The ABTS reactive cation scavenging capacity was assessed by quantifying the absorbance at a wavelength of 734 nm [33]:

$$\text{ABTS}^{\cdot+}\text{scavenging activity } (\%) = [1 - (Ab_{sample}/Ab_{control})] \times 100.$$

2.4.4 Nitric oxide (NO) assay

NO scavenging was carried out, according to Balakrishnan *et al.* [34]. The reaction mixture contained 0.5 mL of PBS and 2 mL of 10 mM sodium nitroprusside (pH = 7.4). About 0.5 mL of 100–1,000 μg·mL^{-1} EPS was added to the reaction mixture, which was then shaken and incubated for 2 h at room temperature. A 0.5 mL sample of the combination was mixed with 1 mL of 0.33% sulfanilic acid in a separate test tube and kept at 37°C for 5 min. Then, 1 mL of 0.1% naphthalene diamine chloride was added and incubated at room temperature for 30 min. The absorbance was recorded at 540 nm [34]:

$$NO\ (\%) = [100 - (Ab_{sample} - Ab_{blank}) \times 100]/Ab_{Control}.$$

2.4.5 Total antioxidant (TAC) assay

EPS evaluation was conducted using spectrophotometric analysis based on the phosphomolybdenum technique. About 1 mL of 0.5 mg·mL^{-1} EPS was mixed with 3 mL of reagent solution containing 0.6 M H_2SO_4, 28 mM NaH_2PO_4, and 4 mM ammonium molybdate. A blank was prepared with only 4 mL of the reagent solution. The samples and blank were heated at 95°C for 150 min and then cooled to room temperature [35]. The absorbance at a wavelength of 630 nm was quantified using a microtiter plate reader (Biotek ELX800, VT, USA). The values were quantified using the ascorbic acid equivalent (AAE) unit, expressed in μg·mg^{-1} of EPSF8, as described by Lahmass *et al.* [36].

2.4.6 Ferric reducing antioxidant power (FRAP) assay

To examine the influence of solvent polarity on the total reducing power of the EPS, the potassium ferricyanide ($K_3Fe(CN)_6$) and trichloroacetic acid ($C_2HCl_3O_2$) method was used as described by Benzie and Strain [37] with certain adjustments and modifications to accommodate the microplate technique, as outlined by Athamena *et al.* [38]. In brief, 40 mL of EPS was added to a tube with 50 mL of 0.2 M Na_2HPO_4 buffer, 50 mL of 1% $K_3Fe(CN)_6$, and 50 mL of 10% CCl_3COOH acid. The mixture was centrifuged at 3,000 rpm for 10 min. Then, 166.66 mL of the supernatant and 33.3 mL of 1% $FeCl_3$ were added to wells. The readings were recorded at 630 nm *via* a microtiter plate reader (Biotek ELX800; Biotek, Winooski, VT, USA). DMSO was employed as the negative control in the experimental setup, while ascorbic acid at 1 mg·mL^{-1} was the positive control. The outcomes were quantified regarding AAE μg·mg^{-1} of the sample.

2.5 Anti-inflammatory evaluation of the ESP

2.5.1 *In vitro* inhibition of 5-lipoxygenase (5-LOX) activity

LOX solution (1,000 U·mL^{-1}, pH = 9) was mixed with varying concentrations of EPS (0.98–125 μg·mL^{-1}) for 15 min at room temperature. After adding linoleic acid, the reaction was measured by monitoring absorption at 234 nm using a microplate reader (BIOTEK, Winooski, VT, USA) [39] with ibuprofen as the positive control:

$$\text{5-LOX Inhibition } (\%) = (1 - Ab_{\text{Sample } 234}/Ab_{\text{Control } 234}) \times 100.$$

2.5.2 *In vitro* inhibition of cyclooxygenase (COX-2) activity

The efficacy of EPS in alleviating inflammation was assessed through its capacity to inhibit the COX-2 enzyme (0.98–125 μg·mL^{-1}) compared to the reference standard (0.98–125 μg·mL^{-1} Celecoxib) following a methodology outlined by Amessis-Ouchemoukh *et al.*, which depends on the oxidation of TMPD by arachidonic acid in the presence of COX-2 enzyme [40]. The inhibitory activity percentage of the EPS against the COX-2 enzyme was determined by measuring absorbance at 611 nm using a microplate reader:

$$\text{COX-2 inhibition } (\%) = (1 - Ab_{\text{sample } 611}/Ab_{\text{control } 611}) \times 100.$$

2.6 Butyrylcholinesterase (BChE) inhibition assay

BChE inhibition assay was performed using butyrylcholine iodide as a substrate, based on a colorimetric method outlined

by Gorun *et al.* [41], and final concentrations (0.195–100 μg·mL^{-1}) for the tested EPS were compared with those of rivastigmine control drug (0.195–100 μg·mL^{-1}). BChE was dissolved in 20 mM sodium phosphate buffer (pH = 7.6) to make a 3.47 unit·mL^{-1} stock solution and stored at −80°C. EPS was prepared by dissolving compounds to 100 μg·mL^{-1} in phosphate buffer (pH = 7.6). Solutions were diluted to various concentrations in phosphate buffer before experiments. The 5,5′-dithio-bis-(2-nitrobenzoic acid)–phosphate–ethanol reagent was prepared by dissolving DTNB in ethanol and adding water and phosphate buffer (pH = 7.6) [41]. The absorption was recorded at 405 nm on a microplate reader:

$$\text{BChE inhibition (\%)} = \{(\text{Control}_{405} - \text{Sample}_{405})/\text{Control}_{405}\} \times 100.$$

2.7 Anti-obesity assessment

Anti-lipase inhibition assay was performed using *p*-nitrophenyl butyrate (PNPB) as the substrate for measuring antilipase activity, and lipase stock solutions (1 mg·mL^{-1}) were made in a 0.1 mM K_3PO_4 buffer (pH = 6.0) and kept at −20°C. EPS (1.9, 3.9, 7.8, 15.6, 31.2, 62.5, 125, 250, 500 and 1,000 μg·mL^{-1}) and orlistat of similar concentrations were pre-incubated with lipase for 60 min at 30°C in 0.1 mM KH_2PO_4 buffer) pH = 7.2 in order to determine their lipase inhibitory activity. Then, at a final volume of 100 μL, 0.1 μL of PNPB was added as a substrate to start the reaction. Using a Biosystem 310-plus UV-visible spectrophotometer, the reaction's release of *p*-nitrophenol was quantified at 405 nm after being incubated at 30°C for 5 min [42]:

$$\text{Lipase inhibition (\%)} = 100 - [(B - b)/(A - a) \times 100],$$

where A is the absorbance of lipase without an inhibitor, a is the absorbance of the negative control (DMSO) without an inhibitor/lipase, B is the absorbance of lipase with an inhibitor, b is the absorbance of the negative control (DMSO) with an inhibitor, without lipase, and DMSO was the negative control, and its activity was examined.

2.8 Antidiabetic assessment

2.8.1 *In vitro* α-amylase inhibition assay

The α-amylase inhibition assay utilized the 3,5-dinitrosalicylic acid (DNSA) method described by Wickramaratne *et al.* [43]. In this assay, EPS was tested at concentrations ranging from 1.95 to 1,000 μg·mL^{-1} and compared to an acarbose standard control at the same concentrations (1.95–1,000 μg·mL^{-1}). About 200 μL of α-amylase solution was combined with 200 μL of EPS and held at 30°C for 10 min. Then, 200 μL of 1% starch solution was added and incubated for 3 min. The reaction was terminated by adding 200 μL of DNSA reagent and boiling for 10 min at 85–90°C. The mixture was cooled to room temperature and diluted with 5 mL of H_2O [43]. The absorbance was recorded at 540 nm using a Biosystem 310 spectrophotometer. The IC_{50} values were obtained from the graph by plotting the percentage of α-amylase inhibition against the EPS concentration:

$$\text{α-amylase inhibition (\%)} = (\text{Abs}_{\text{control}} - \text{Abs}_{\text{Sample}}) \times 100/\text{Abs}_{\text{control}}.$$

2.8.2 *In vitro* α-glucosidase inhibition assay

The α-glucosidase inhibition assay followed Pistia Brueggeman and Hollingsworth's method. EPS at concentrations ranging from 1.95 to 1,000 μg·mL^{-1} was compared to an acarbose control at the same concentrations. EPS (1.97–1,000 μg·mL^{-1}) was incubated with α-glucosidase enzyme solution (1 U·mL^{-1}) for 20 min. After 20 min, 1 M pNPG substrate was added and incubated for 30 min. The reaction was terminated by adding 0.1 N Na_2CO_3 [44]. Absorbance was scaled at 405 nm using a Biosystm 310 plus spectrophotometer. The IC_{50} values were evaluated using a regression equation derived from graphing concentrations ranging from 1.95 to 1,000 μg·mL^{-1} against the corresponding % of inhibition.

$$\text{α-glucosidase (\%)} = (\text{OD}_{\text{control}} - \text{OD}_{\text{blank}})/\text{OD}_{\text{blank}} \times 100.$$

2.9 Antimicrobial evaluation

The EPS was tested as an antimicrobial compound by agar well diffusion approach against the following bacterial ATCC spectrum, G +ve *Bacillus subtilis* (ATCC 6633), *Staph. aureus* (ATCC 6538), and *Enterococcus faecalis* (ATCC 10541). G −ve bacteria were *E. coli* (ATCC 8739), *K. pneumoniae* (ATCC13883), and *Salmonella typhi* (ATCC 6539). An inoculum suspension was adjusted for the broth dilution standard protocol, and inoculated agar plates were within 15 min. All dried agar was streaked in three directions. After drying the agar for 15 min, a hole with a 6–8 mm diameter is punched aseptically with a sterile cork borer or a tip. EPSF8 and gentamicin were the reference drugs dissolved in MDSO at 10 mg·mL^{-1}. Then, 100 ml of EPSF8 was added to the well at the required concentration. Within 15 min of disposal, plates were incubated for 16–48 h, and the inhibition zone widths (in mm) around the wells were measured to the nearest full millimeter at the moment of significant growth reduction [45].

Minimum inhibitory concentrations (MICs) and minimum bactericidal concentrations (MBCs) were investigated following the Clinical and Laboratory Standards Institute (CLSI) [46].

2.10 Antibiofilm assessment

We assessed how EPS affected the production of biofilms in 96-well polystyrene flat-bottom plates. In summary, 300 µL of trypticase soy yeast broth with a final concentration of 10^6 CFU·mL^{-1} was cultivated in sublethal doses of 75, 50, and 25% of MBC. After 48 h of incubation at 37°C, the biofilm grown on the plates was dyed for 15 min at 37°C using a 0.1% crystal violet aqueous solution. The excess stain was removed from the plate with sterile dH_2O after incubation. Each well received 250 µL of 95% C_2H_5OH to solubilize the dye attached to the cells. A microplate reader was used to measure the absorbance at 570 nm after 15 min [47]:

$$\text{Biofilm inhibition (\%)} = [1 - (Ab_{sample} - Ab_{blank})/(Ab_{control} - Ab_{blank}] \times 100.$$

2.11 Statistical analysis

The data were analyzed using one-way ANOVA and Duncan's test for multiple concentration comparisons. Normal distribution was confirmed with Kolmogorov–Smirnov and Shapiro–Wilk tests. Statistical analyses were performed using SPSS v25 with a significance level of $P \leq 0.05$ and a sample size of $n = 3$ in triplicates.

3 Results

3.1 Isolation and phylogenetic analysis of the EPS-producing bacterial isolate

Ten bacterial isolates were collected from the Red Sea and subjected to screening for EPS synthesis. This screening process involved evaluating their cultural properties and morphological characteristics and measuring the yield of EPS production. The marine bacterium (F8) strain was found to be the highest EPS producer (6.98 g·L^{-1}), with a main fraction of 82.4%. The selected strain was studied microbiologically, and it was a G −ve, non-capsulated, and non-spore-forming bacterium (Table S1). In addition, the strain was studied biochemically and physiologically. It was positive for the following tests (catalase, citrate, oxidase, nitrate reduction, and mannitol) and negative for the rest of the tests (Table S2).

Molecular 16S rRNA sequencing was then carried out, and the phylogenetic tree involved a comparative analysis of sequences that exhibited a significant level of resemblance between the rRNA sequences of the chosen bacterium under investigation. The obtained rRNA gene sequences were

Figure 1: Phylogenetic tree analysis of *Pseudomonas* sp. strain AHG22 based on 16S rRNA gene sequencing.

observed to correspond to *Pseudomonas* sp. strain AHG22 (Figure 1), indicating that the tree was generated correctly. Confirmation of the identification of *Pseudomonas* sp. strain AHG22 was established using the accession number (OQ931874). The BLAST tool was employed to analyze the provided DNA sequence, which was subsequently submitted to the NCBI GenBank database.

3.2 Production, partial purification, and chemical composition analysis of EPSF8

The F8 bacterial strain synthesized EPS (EPSF8) with a yield of 6.98 g·L^{-1}. Subsequently, EPSF8 was subjected to UV absorption spectra in the range of 200–800 nm (Figure S1) and had no protein when tested by FT-IR spectroscopy, where the broad characteristic peak at 3588.17 cm^{-1} was assigned to OH^{-1} stretching vibration. The band at 2933.66 cm^{-1} was correlated with the stretching vibration of C–H in the sugar ring. Also, the absorption at 1619.88 cm^{-1} referred to COO^{-} vibration and 1292.29 cm^{-1} to the symmetrical COO^{-} stretching vibration, which proved the presence of uronic acid. The band at 1081.53 cm^{-1} indicated the SO_3 group and was characteristic absorption at 853.94 cm^{-1} arising from β-configuration of the sugar units (Figure 2).

The HPLC chromatogram of EPSF8 revealed the monosaccharides fractions (glucose:galacturonic acid: xylose:rhamnose) with a molar ratio of 1:2:2:3, respectively (Figure 3).

3.3 Antioxidant evaluation of EPSF8

The efficacy of EPSF8 in scavenging DPPH radicals was evaluated at 1.95–1,000 μg·mL^{-1} doses. The DPPH scavenging percentage is enhanced by increasing EPSF8 concentrations from 62.5 to 1,000 μg·mL^{-1}. At its lowest tested concentration of 1.95 μg·mL^{-1}, EPSF8 scavenged 14.8% of DPPH radicals, increased progressively with higher concentrations, reaching 22.7% at 3.9 μg·mL^{-1}, 30.7% at 7.8 μg·mL^{-1}, 37.2% at 15.6 μg·mL^{-1}, and 45.3% at 31.2 μg·mL^{-1}. The scavenging peaked at 84.2% at the highest tested concentration of 1,000 μg·mL^{-1}. The IC_{50} value of EPSF8 against DPPH was calculated as 46.99 μg·mL^{-1} (Figure 4) compared to ascorbic acid (IC_{50} = 2.52 μg·mL^{-1}) (Figure S2). For H_2O_2 assessment, the maximum antioxidant activity was 77.03 ± 1.20% after 1 h at 1,000 μg·mL^{-1}, and the IC_{50} value was 300 μg·mL^{-1} after 60 min (Figure 5) compared to control (IC_{50} = 88.71 ± 0.98 μg·mL^{-1}) (Table S3). Similarly, the maximum activity for ABTS$^{\cdot+}$ was found after 60 min to be 67.30 ± 1.12% at 1,000 μg·mL^{-1}, and IC_{50} was 300 μg·mL^{-1} after 1 h (Figure 6) compared to ascorbic acid (IC_{50} = 87.50 ± 0.75 μg·mL^{-1}) as control (Table S3). For NO antioxidant assessment, the maximum activity (74.34 ± 1.08%) was recorded after 1 h at 1,000 μg·mL^{-1}, and the IC_{50} was detected at 100 μg·mL^{-1} after 60 min (Figure 7) compared to the control (IC_{50} = 20.81 μg·mL^{-1}) (Table S4). The TAC of EPSF8 showed a TAC of 219.45 μg·mg^{-1} AAE. At the same time, the FRAP assay also determined the antioxidant capacity of EPSF8 to be 54.15 μg·mg^{-1} AAE. All data are presented as mean ± SD (n = 3, P < 0.05).

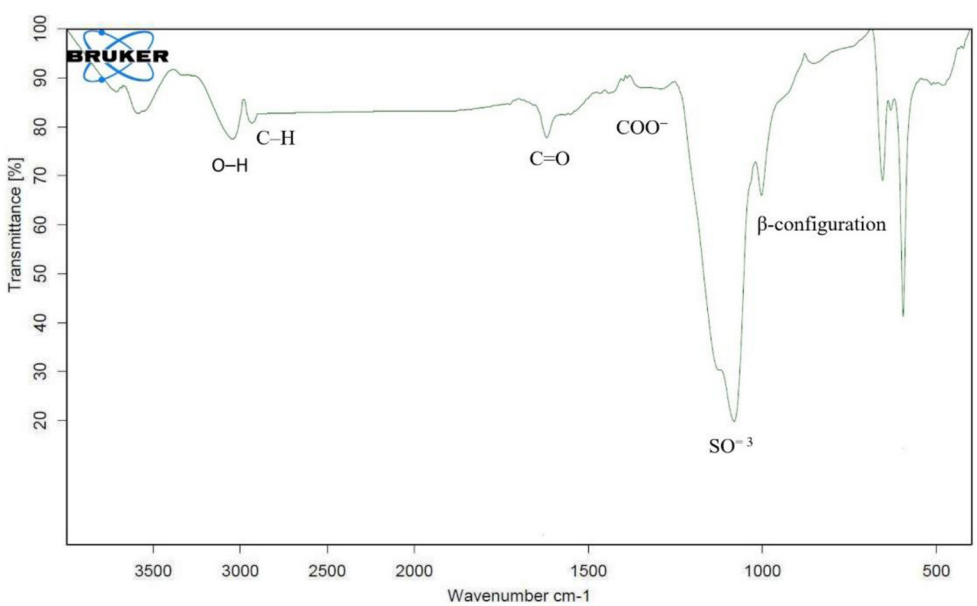

Figure 2: FTIR spectra of EPSF8 displaying the main functional groups.

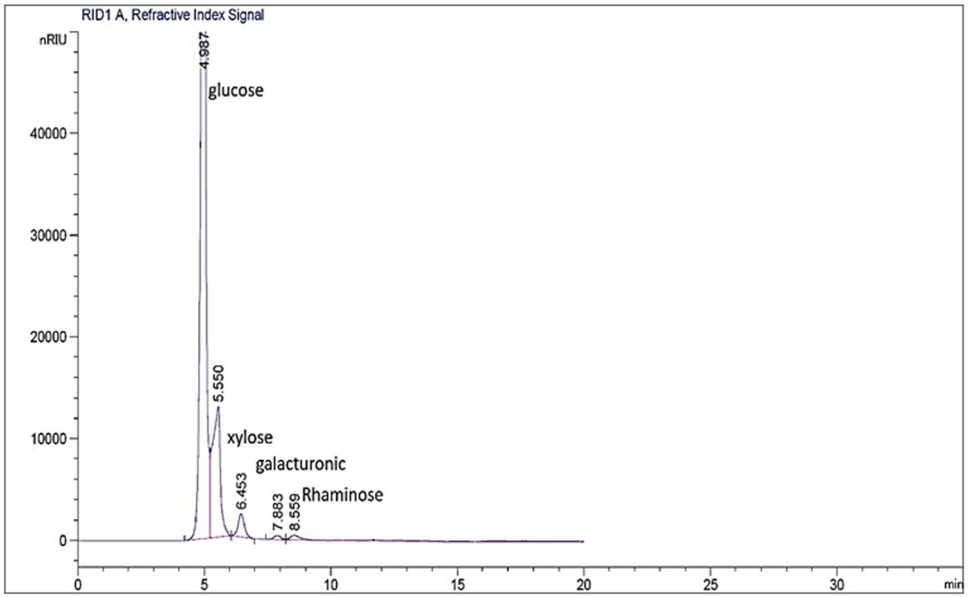

Figure 3: HPLC chromatogram of the EPSF8 from *Pseudomonas* sp. strain AHG22.

3.4 Anti-inflammatory assessment of EPSF8

The ability of EPSF8 to reduce inflammation was estimated by investigating its *in vitro* inhibition effects against both COX-2 and 5-LOX. At the lowest concentration of 0.98 μg·mL^{-1}, EPSF8 inhibited LOX by 11.45%. The inhibition increased progressively with higher concentrations, reaching 17.93% at 1.95 μg·mL^{-1}, 29.30% at 3.9 μg·mL^{-1}, 46.02% at 7.81 μg·mL^{-1}, and 54.16% at 15.63 μg·mL^{-1}. Potent LOX inhibition started at 31.25 μg·mL^{-1}, where 65.87% inhibition was observed. EPSF8 displayed its maximum LOX inhibitory activity of 79.54% at the highest tested concentration of 125 μg·mL^{-1} (Figure 8). The IC_{50} value for EPSF8 on 5-LOX was 14.82 compared to that of ibuprofen (1.5 ± 1.3 μg·mL^{-1}; Table S5).

For *in vitro* inhibition of COX-2, at 0.98 μg·mL^{-1}, EPSF8 inhibited COX-2 by 12.73%. The inhibition increased progressively with higher concentrations, reaching 21.94% at 1.95 μg·mL^{-1}, 30.52% at 3.9 μg·mL^{-1}, 43.74% at 7.81 μg·mL^{-1}, and 52.98% at 15.63 μg·mL^{-1}. Potent COX-2 inhibition started at 31.25 μg·mL^{-1}, where 61.90% inhibition was observed. EPSF8 displayed its maximum COX-2 inhibitory activity of 86.33% at the highest tested concentration of 125 μg·mL^{-1} (Figure 8). The IC_{50} value of EPSF was 15.49 μg·mL^{-1} compared to that of celecoxib (0.28 ± 1.7 μg·mL^{-1}; Table S6). A positive correlation

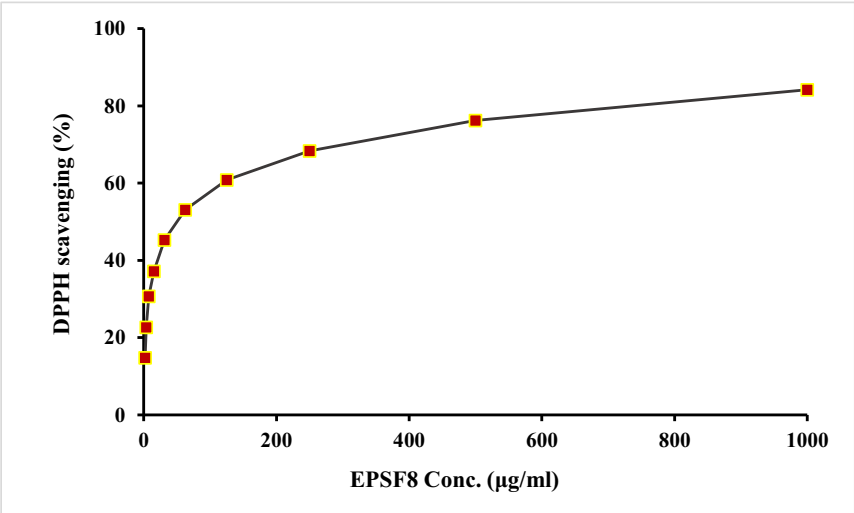

Figure 4: DPPH radical scavenging by EPSF8 (1.95–1000 μg/ml) increased dose-dependently. Data are shown as mean ± SD. One-way ANOVA was utilized for data analysis (n = 3, P < 0.05).

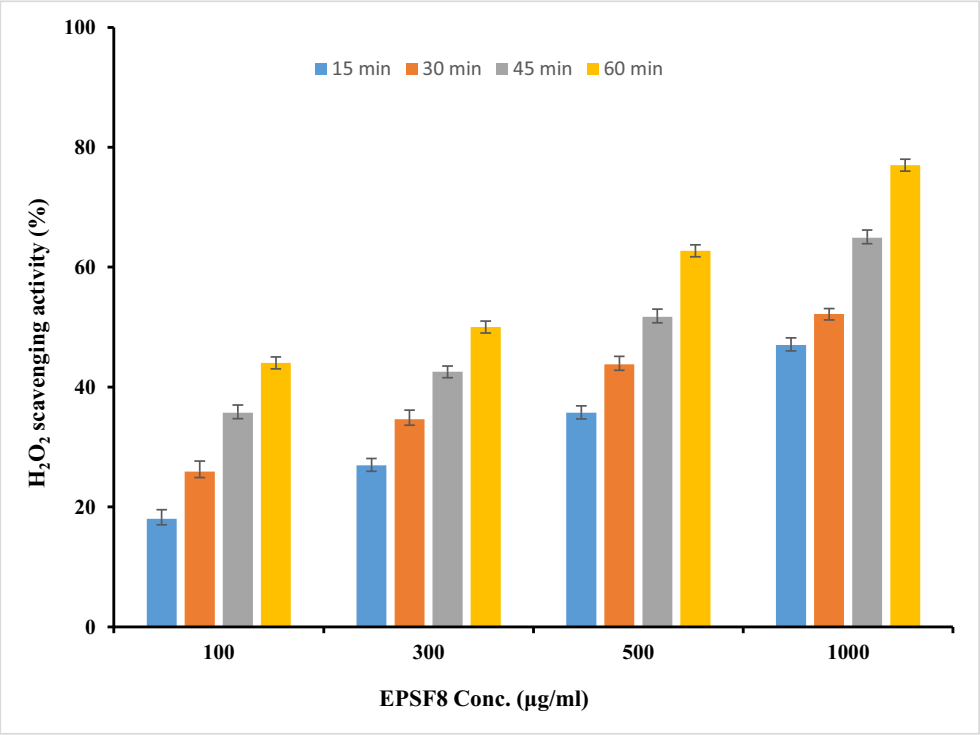

Figure 5: Dose- and time-dependent H_2O_2 scavenging activity of EPSF8. Results expressed as mean ± SD (n = 3, p < 0.05).

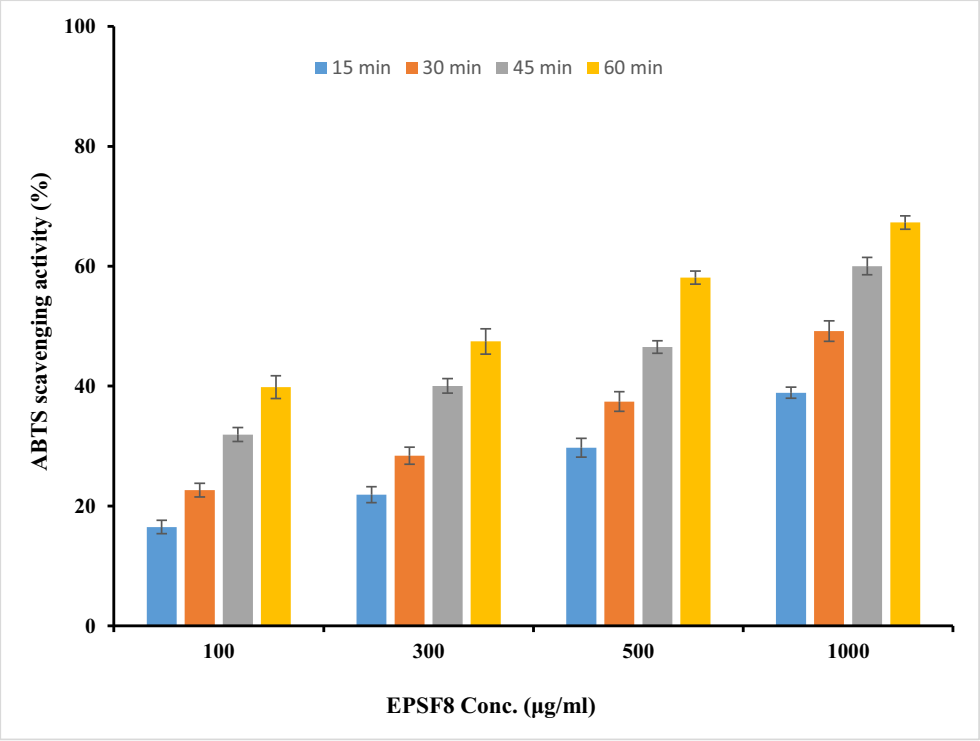

Figure 6: Concentration-dependent ABTS•+ radicals' cation scavenging activity of EPSF8 (100–1000 µg/ml). Values represent mean ± SD (n = 3).

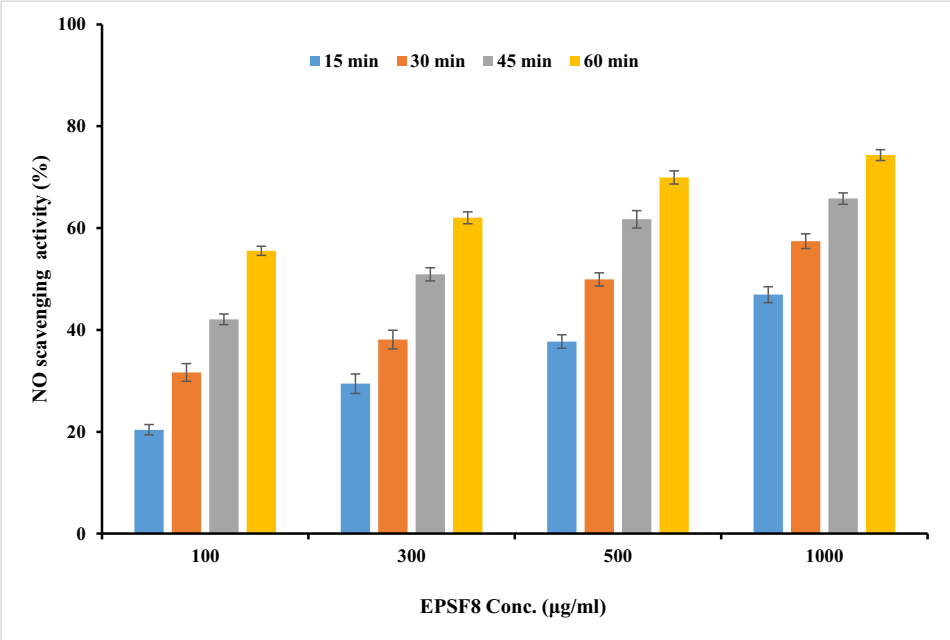

Figure 7: Nitric oxide (NO) radical scavenging activity of EPSF8 (100-1000 µg/ml) and time intervals (15-60 min). Data are presented as mean ± SD (n = 3).

between the increasing concentration of EPSF8 and the extent of inhibition was observed in both enzymatic activities.

3.5 BChE inhibition by EPSF8

Different concentrations (0.195–100 µg·mL^{-1}) of EPSF8 were tested against BChE, and the results were compared to rivastigmine, a control drug. Minimal inhibition of 0.2% was observed at the lowest tested concentration of 0.195 µg·mL^{-1}. The inhibition increased progressively as the concentration of EPSF8 increased, with 12.2% inhibition starting to be observed at 1.56 µg·mL^{-1}. EPSF8 exhibited its maximal inhibitory activity of 83% against BChE at the highest tested concentration of 100 µg·mL^{-1}. In between the lowest and highest concentrations, the inhibition ranged from 1.3% at 0.39 µg·mL^{-1} up to 73.3% at 50 µg·mL^{-1}, showing a steady dose-dependent increase in BChE inhibition by EPSF8. IC_{50} values for EPSF8 and rivastigmine were 11.36 and 2.91 µg·mL^{-1}, respectively (Figure 9 and Figure S5).

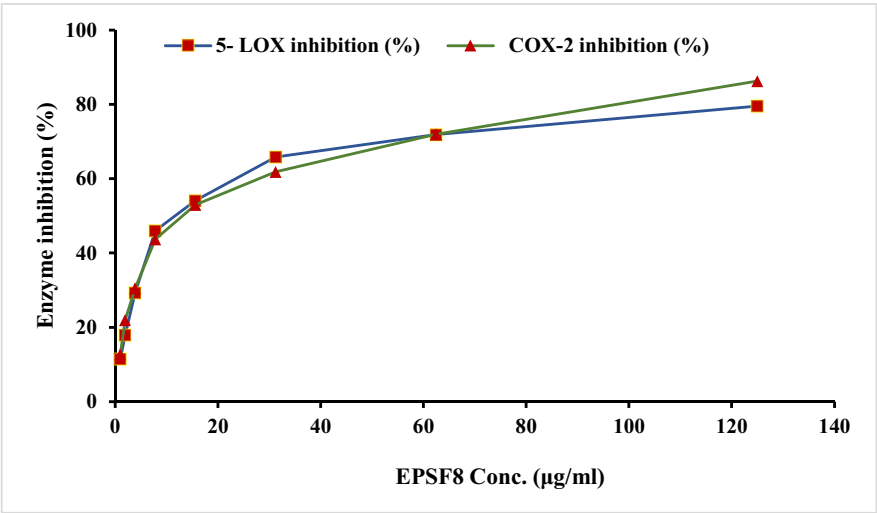

Figure 8: EPSF8 dose-dependently inhibits 5-LOX and COX-2. EPSF8 concentrations increased inflammatory enzyme inhibition. Data is shown as mean ± SD (n = 3). Significant differences between means were determined at $p < 0.05$ using one-way ANOVA.

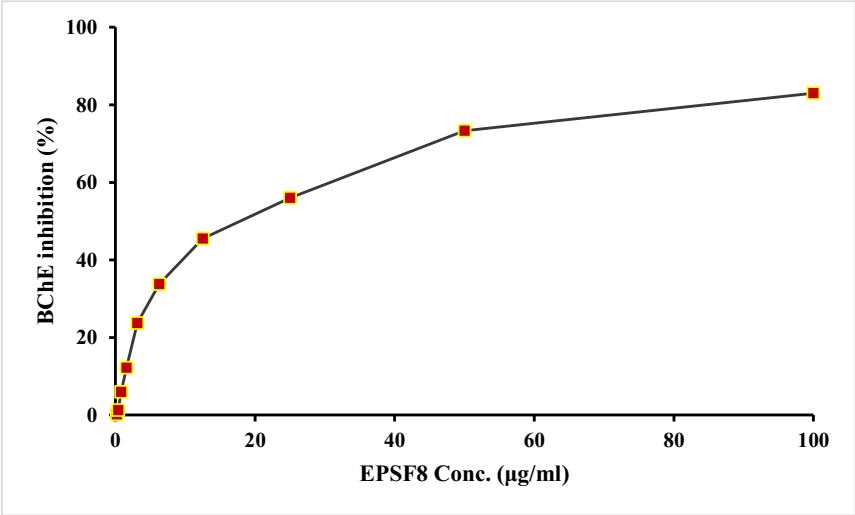

Figure 9: *In vitro* inhibition of BChE by EPSF8 at increasing concentrations. Results are presented as mean ± SD (n = 3). One-way ANOVA determined statistical significance ($p < 0.05$) between means.

3.6 Anti-obesity assessment of EPSF8

The inhibitory effect of EPSF8 against lipase at different concentrations (1.95–1,000 µg·mL^{-1}) was compared with orlistat at the same concentrations. It was observed that the enzyme inhibition increased as the EPSF8 concentration increased. A minimal lipase inhibition of 3.7% was observed at the lowest tested concentration of 1.95 µg·mL^{-1}. The inhibition increased progressively as the concentration increased, reaching 14.8% at 3.9 µg·mL^{-1}, 25% at 7.81 µg·mL^{-1}, 36.3% at 15.62 µg·mL^{-1}, and 37.7% at 31.25 µg·mL^{-1}. Potent lipase inhibition started around 62.5 µg·mL^{-1}, where 48.2% inhibition was attained. At the highest tested concentration of 1,000 µg·mL^{-1}, EPSF8 exhibited its maximal lipase inhibitory activity of 92.6%. The IC_{50} values for EPSF8 and orlistat were calculated to be 56.12 and 20.08 µg·mL^{-1}, respectively (Figure 10 and Figure S6).

3.7 Antidiabetic activity of EPSF8

The DNSA method was carried out to investigate whether EPSF8 could act as a natural antidiabetic drug, and the inhibition assay was carried out against α-amylase and α-glucosidase enzymes. EPSF8 was tested at different concentrations for both enzymes (1.95–1,000 µg·mL^{-1}), and the same range was used for acarbose, which served as the

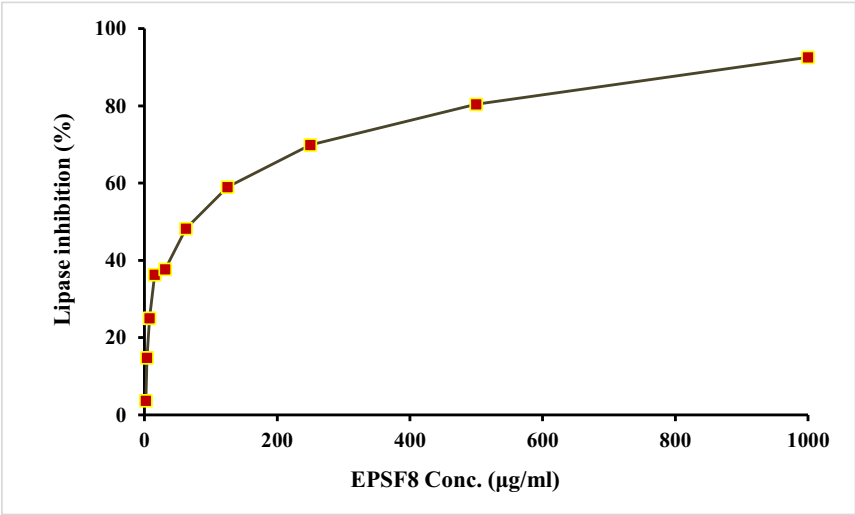

Figure 10: *In vitro* dose-dependent inhibition of pancreatic lipase by EPSF8. Mean ± SD (n = 3). Differences were significant at $p < 0.05$ by one-way ANOVA.

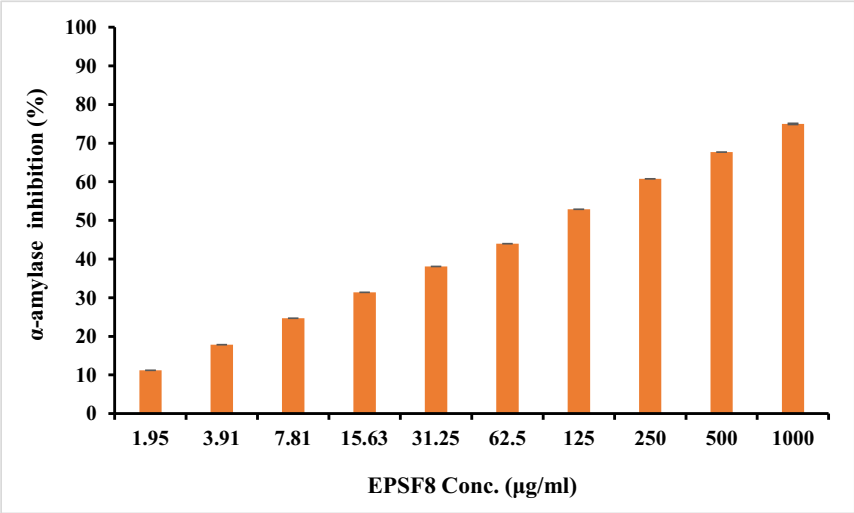

Figure 11: Dose-dependent inhibition of α-amylase by EPSF8. Elevated EPSF8 concentrations correlated with higher α-amylase inhibition. Results are shown as mean ± SD (n = 3). One-way ANOVA was used to determine statistical significance at $p < 0.05$ for mean differences.

control used in this experiment. At 1.95 µg·mL^{-1}, EPSF8 inhibited amylase by 11.2%. The inhibition increased to 17.8% at 3.91 µg·mL^{-1}, 24.7% at 7.81 µg·mL^{-1}, and 31.4% at 15.62 µg·mL^{-1}, indicating a steady dose-dependent increase in amylase inhibition by EPSF8. The second maximum inhibition of 67.7% was observed at 500 µg·mL^{-1}, and the highest concentration tested at 1,000 µg·mL^{-1} EPSF8, showed the highest inhibition activity of 75% (Figure 11). The IC_{50} of EPSF8 was 93.1 µg·mL^{-1} for *in vitro* α-amylase, and that of acarbose was 50.93 (Figure S7).

On the other hand, EPSF8 exhibited concentration-dependent inhibitory activity against the α-glucosidase enzyme. At the lowest concentration of 1.95 µg·mL^{-1}, EPSF8 inhibited α-glucosidase by 10.2%. The inhibition increased progressively with higher concentrations, reaching 16.7% at 3.91 µg·mL^{-1}, 22.4% at 7.81 µg·mL^{-1}, 30% at 15.63 µg·mL^{-1}, and 35.9% at 31.25 µg·mL^{-1}. Potent α-glucosidase inhibition started at 62.5 µg·mL^{-1}, where 42.2% inhibition was observed. EPSF8 showed its maximum α-glucosidase inhibitory activity of 71% at the highest tested concentration of 1,000 µg·mL^{-1} (Figure 12). Its IC_{50} was 127.28 and 4.13 µg·mL^{-1} for acarbose (Figure S8) (Table S7).

3.8 Antimicrobial and antibiofilm assessment of EPSF8

EPSF8 was supplemented on the Mueller–Hinton agar plate. After incubation, inhibition zones were represented

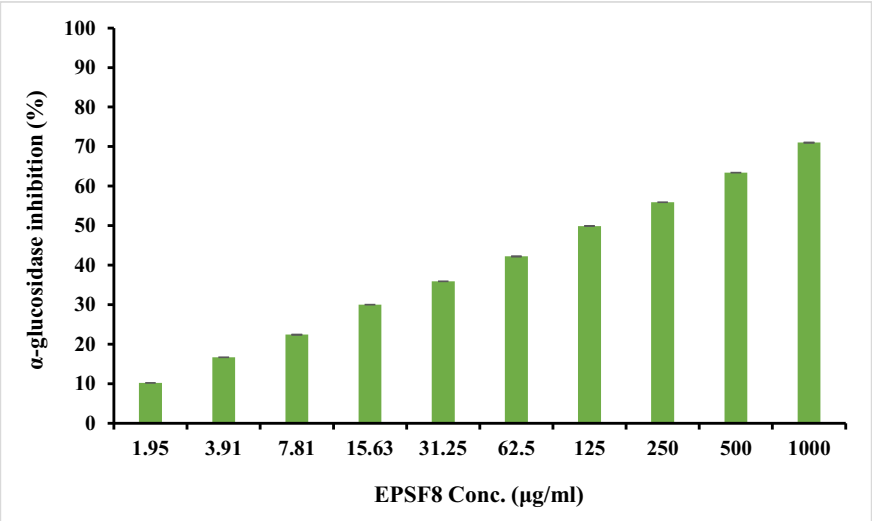

Figure 12: Concentration-dependent α-glucosidase inhibition by EPSF8 with concentrations from 1.95 to 1000 µg/mL (n = 3, $p < 0.05$, one-way ANOVA).

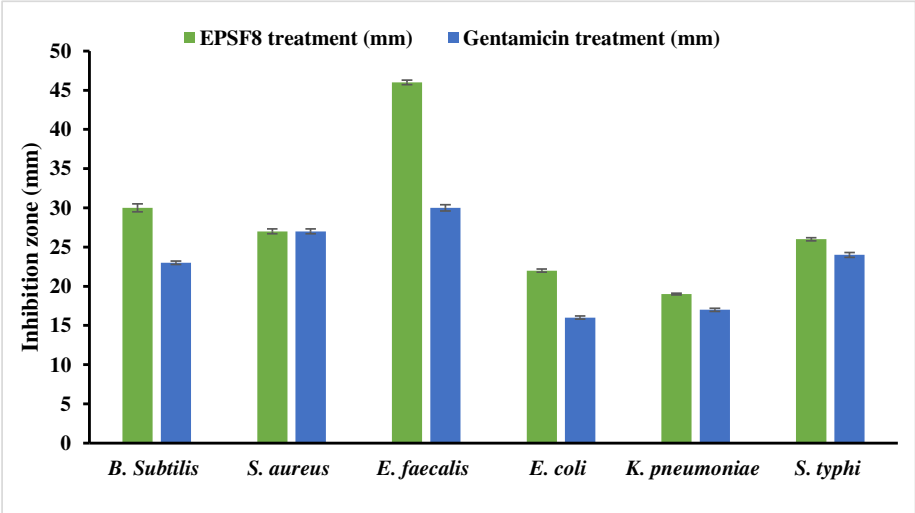

Figure 13: Inhibition zones (mm) of EPSF8 towards G+ve and G-ve ATCC bacteria.

as mm. The tested organisms were G +ve *B. subtilis* (ATCC 6633) *Staph. aureus* (ATCC 6538) and *E. faecalis* (ATCC 29212). G −ve bacteria were *E. coli* (ATCC 8739), *K. pneumoniae* (ATCC13883), *and S. typhi* (ATCC 6539). For the G +ve spectrum, against *B. subtilis*, EPSF8 produced an inhibition zone of 30 ± 0.5 mm, larger than the 23 ± 0.2 mm zone caused by gentamicin. For *S. aureus*, EPSF8 and gentamicin both generated an equal inhibition zone of 27 ± 0.3 mm. However, EPSF8 showed superior inhibition of *E. faecalis*, creating a 46 ± 0.3 mm zone compared to just 30 ± 0.4 mm for gentamicin (Figures 13 and 14). MICs, MBCs, and MBC/MIC ratios were then investigated. Against *B. subtilis*, EPSF8 exhibited the lowest MIC of 15.62 μg·mL^{-1} and a corresponding MBC of 31.25 μg·mL^{-1}, resulting in an MBC/MIC ratio of 2. For *S. aureus*, the MIC and MBC were the same at 15.62 and 31.25 μg·mL^{-1}, respectively, also giving an MBC/MIC ratio of 2, while EPSF8 displayed the highest potency against *E. faecalis* with the lowest MIC of 7.8 μg·mL^{-1} and matched by an MBC of 7.8 μg·mL^{-1}, resulting in an MBC/MIC ratio of 1 indicating bactericidal effects (Table 1).

For the G −ve spectrum, for *E. coli*, EPSF8 produced an inhibition zone of 22 ± 0.2 mm, while gentamicin generated a smaller 16 ± 0.2 mm zone. For *K. pneumoniae*, inhibition zones were comparable at 19 ± 0.1 mm for EPSF8 and 17 ± 0.2 mm for gentamicin. EPSF8 exhibited the strongest inhibition of *S. typhi*, creating a 26 ± 0.2 mm zone compared to 24 ± 0.3 mm for gentamicin (Figures 13 and 15). Following MICs, MBCs, and MBC/MIC ratios were examined; against *E. coli*, EPSF8 displayed the highest MIC of 125 μg·mL^{-1} and a matching MBC of 125 μg·mL^{-1}, resulting in an MBC/MIC ratio of 1. For *K. pneumoniae*, the MIC was the same at 125 μg·mL$^{-1,}$ but the MBC was slightly higher at 250 μg·mL^{-1}, giving an MBC/MIC ratio of 2. EPSF8 exhibited the greatest potency against *S. typhi* with the lowest MIC of 62.5 μg·mL^{-1} and a MBC of 125 μg·mL^{-1}, resulting in an MBC/MIC ratio of 2 (Table 1).

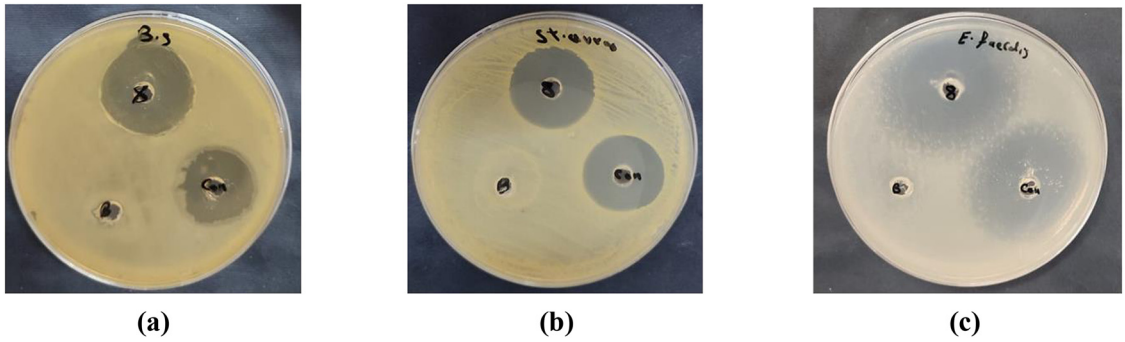

Figure 14: Antibacterial effect of EPSF8 against 3 ATCC G+ve pathogenic bacteria (a) *B. subtilis*, (b) *S. aureus*, and (c) *E. faecalis*.

Table 1: Inhibition zones (in mm), MIC, MBC, and MBC/MIC ratio of EPSF8 against 6ATCC bacteria

Pathogenic microorganisms	EPSF8 (mm)	Gentamicin (control)	MIC (μg·mL^{-1})	MBC (μg·mL^{-1})	MBC/MIC ratio
B. subtilis (ATCC 6633)	30 ± 0.5	23 ± 0.2	15.62	31.25	2
Staph. aureus (ATCC 6538)	27 ± 0.3	27 ± 0.3	15.62	31.25	2
E. faecalis (ATCC 29212)	46 ± 0.3	30 ± 0.4	7.8	7.8	1
E. coli (ATCC 8739)	22 ± 0.2	16 ± 0.2	125	125	1
K. pneumoniae (ATCC13883)	19 ± 0.1	17 ± 0.2	125	250	2
S. typhi (ATCC 6539)	26 ± 0.2	24 ± 0.3	62.5	125	2

For the same bacterial spectrum except for *E. coli*, EPSF8 was tested as antibiofilm based on the previously addressed MIC and MBC values (Figure 16). For G +ve bacteria, EPSF8 showed the lowest antibiofilm activity, 91.89% for *Staph. aureus* at 75% of MBC. Conversely, the highest antibiofilm activity was 93.47% for *E. faecalis*. On the other hand, for G −ve bacteria, EPSF8 exhibited the lowest activity (87.91%) for *K. pneumoniae* and the highest (91.79%) for *S. typhi*.

4 Discussion

Microbial EPSs exhibit a remarkable range of diversity. Multifunctional carbohydrates evidenced a diverse range of physiological responses, thereby showcasing their noteworthy potential in augmenting public health. Currently, a substantial portion of marketable EPSs can be attributed to the derivation of microorganisms. One primary advantage of EPSs lies in their inherent capacity for modulating chemical composition and structure. This characteristic renders them particularly well-suited for targeted applications within pharmaceuticals and medicine.

Henceforth, the main goal of this study was to identify microbial EPSs possessing chemically suitable architectures, which has been pursued *via* comprehensive screening investigations conducted within untapped marine ecosystems.

A marine bacterium *Pseudomonas* sp. strain AHG22 was isolated and identified (Figure 1), which produced EPS with a yield of 6.98 g·L^{-1} with a core fraction (82.4%), and coded EPSF8. The EPSF8 was then subjected to FT-IR and revealed uronic acid (14.70%), sulfate (25.65%), and N-acetyl glucosamine (8.55%) (Figure 2). HPLC chemical investigation revealed monosaccharide fractions (glucose: galacturonic acid:xylose:rhamnose) with molar ratios 1:2:2:3, respectively (Figure 3).

At different concentrations, the antioxidant activity of EPSF8 was investigated by DPPH, H_2O_2, ABTS$^{\cdot+}$, NO, TAC, and FRAP assay. For DPPH radical scavenging activity, IC_{50} values of EPSF8 and the standard compound ascorbic acid were determined to be 46.99 and 2.52 μg·mL^{-1}, respectively (Figure S2). The EPSF8 extract displayed the highest antioxidant at a concentration of 1,000 μg·mL^{-1}; EPSF8 exhibited 77.03 ± 1.20 μg·mL^{-1} of antioxidant activity in the H_2O_2 assay after 60 min (Figure 5). EPSF8 also showed 67.30 ± 1.12 μg·mL^{-1} of antioxidant activity in the ABTS$^{\cdot+}$ assay after 60 min (Figure 6). In addition, for NO assay, EPSF8 yielded maximum activity (74.34 ± 1.08 μg·mL^{-1}) after 1 h at a 1,000 μg·mL^{-1} concentration (Figure 7). All the antioxidant activities measured in the H_2O_2, ABTS$^{\cdot+}$, and NO assays positively correlated with the tested concentration values.

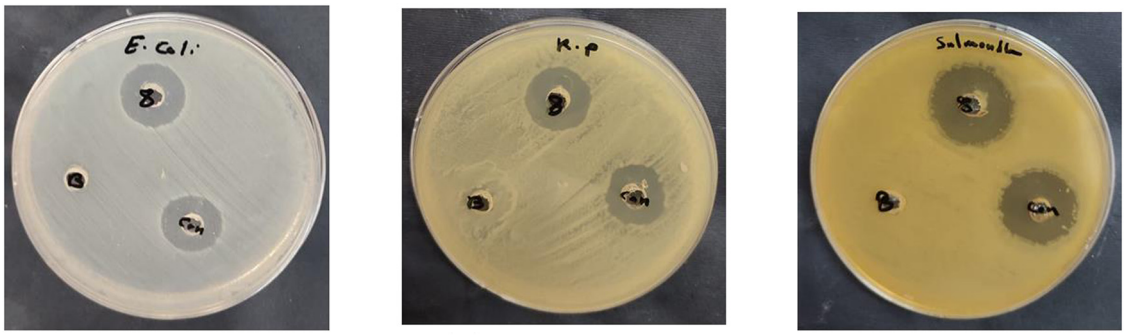

(a) (b) (c)

Figure 15: Antibacterial effect of EPSF8 against 3 ATCC G-ve pathogenic bacteria. (a) *E. coli*, (b) *K. pneumoniae*, and (c) *S. typhi*.

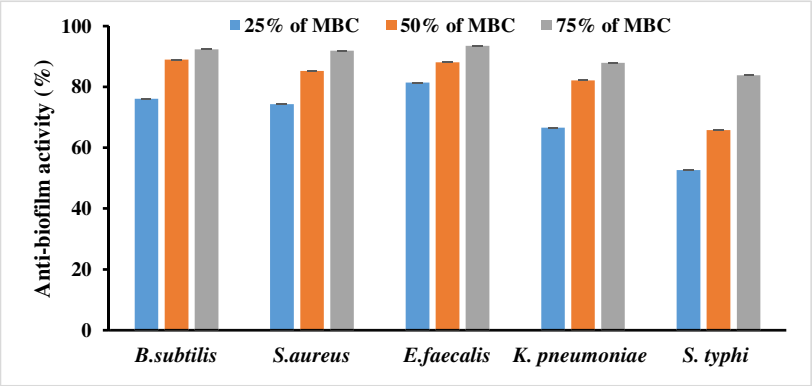

Figure 16: Antibiofilm activity of EPSF8 against ATCC bacteria at different %MBC.

For the TAC assay, EPSF8 had 219.45 μg·mg^{-1} equivalent AAE and 54.15 μg·mg^{-1} AAE for FRAP testing.

The antioxidant efficiency of microbial EPS has been explored primarily by *in vitro* assays [6–9]. Multiple factors, such as monosaccharide molar ratio, molecular weight, or functional groups, may potentially influence the EPS's antioxidant activity. In addition, the techniques employed for extraction and purification may also have an impact. The low molecular weight EPSs that are acidic polymers, as in the case of the current EPSF8, frequently displayed greater antioxidant capabilities than the neutral ones [48].

Therefore, EPSF8 could be regarded as a potentially green alternative agent against synthetic antioxidants due to its involvement in mitigating oxidative stress by scavenging different free radicals, inhibiting lipid peroxidation, and reducing the activity of metal ions. However, to confirm these data, the activity of EPSF8 should be supported by *in vivo* tests.

The enzymes 5-LOX and COX-2 are key targets in developing anti-inflammatory drugs. This is because they play a vital role in regulating the production of leukotrienes and prostaglandins – important inflammatory mediators. By attenuating the activity of these enzymes, it is possible to mitigate the inflammatory response and potentially alleviate associated symptoms [49]. We explored the anti-inflammatory potency of EPSF8 by evaluating it against 5-LOX and COX-2 enzymes.

Our current findings revealed that EPSF8 had an IC_{50} of 14.82 μg·mL^{-1} for inhibiting 5-LOX activity (Figure 8), compared to an IC_{50} of 1.5 ± 1.3 μg·mL^{-1} for ibuprofen (Table S5). EPSF8 also had an IC_{50} of 15.49 μg·mL^{-1} for inhibiting COX-2 activity (Figure 8), compared to an IC_{50} of 0.28 ± 1.7 μg·mL^{-1} for celecoxib. As observed, increasing the concentration of EPSF8 resulted in a dose-dependent elevation in inhibiting 5-LOX and COX-2 activities. The prevailing notion posits that the primary impact of EPS lies in its ability to regulate cytokines and their subsequent transcription factors [50]. The pro-inflammatory cytokines TNF-α, IL-1, and IL-6, along with the anti-inflammatory cytokine IL-10, have been identified as the key mediators responsible for the effects exerted by these natural products [51].

BChE is an enzyme categorized as nonspecific cholinesterase that catalyzes the hydrolysis of choline-based esters. By hydrolyzing acetylcholine (ACh), BChE plays a crucial part in preserving appropriate cholinergic function, similar to acetylcholinesterase (AChE) [52]. The implementation of targeted inhibition of BChE has been widely acknowledged as a promising therapeutic strategy in the context of Alzheimer's disease [53]. Therefore, in pursuit of further elucidation to explore some bacterial *in vitro* anti-BChE activity, EPSF8 was tested for anti-BChE activity at concentrations ranging from 0 to 100 μg·mL^{-1}. EPSF8 had an IC_{50} of 11.36 μg·mL^{-1} against BChE (Figure 9), compared to an IC_{50} of 2.91 μg·mL^{-1} for the rivastigmine control (Figure S5). Recent scientific investigations have revealed the neuroprotective properties of secondary metabolites derived from marine bacteria. For example, EPSF6, EPS with Mw of 2.7 × 10^4 g·mol^{-1} sourced from *Bacillus Velezensis* AG6 had an anti-AChE activity with IC_{50} (100–1,000 μg·mL^{-1}) = 439.05 μg·mL^{-1} compared to that of the eserine control (0.02–0.12 μg·mL^{-1}) = 0.09 μg·mL^{-1} [9]. From the same source, EPSR5, an acidic EPS with an Mw of 4.9 × 10^4 g·mol^{-1} extracted from *Kocuria* sp., revealed the anti-AChE activity with IC_{50} = 797.02 μg·mL^{-1} compared to that of eserine's of 0.09 μg·mL^{-1} [8]. Also, pyrroles and other AChE inhibitors were generated by *Streptomyces lateritius* [54]. In addition, Gangalla *et al.* have documented the potential therapeutic impact of a polysaccharide sourced from *Bacillus amyloliquefaciens* RK3 in mice. This finding holds promise for treating various disorders driven by ACh insufficiency [55].

Empirical investigations have demonstrated that the inhibitory impact of COX-2 diminishes the inflammatory cascade, thereby exerting a noteworthy influence on the neurodegenerative processes associated with the progression of Alzheimer's disease [56]. In light of its current attributes, EPSF8 exhibited selective anti-cyclooxygenase properties, inhibited BChE, and possessed antioxidant capabilities. These characteristics position EPSF8 as a potentially advantageous acidic microbial polysaccharide for controlling and restricting Alzheimer's disease.

To assess the anti-obesity potential of EPSF8 through lipase enzyme inhibition, EPSF8 was tested at concentrations ranging from 1.95 to 1,000 $\mu g \cdot mL^{-1}$ compared to similar concentrations of the Orlistat control. The IC_{50} of EPSF8 for lipase inhibition was 56.12 $\mu g \cdot mL^{-1}$ (Figure 10) compared to 20.08 $\mu g \cdot mL^{-1}$ for orlistat (Figure S6). Microbial EPS's hypoglycemic and cholesterol-lowering efficiency has been confirmed mainly through *in vitro* experiments [57,58]. Although the precise mechanisms underlying the EPS's ability to decrease cholesterol are still unclear, it has been speculated that they do so by acting like dietary fibers and promoting the synthesis of bile acids [59]. Additionally, the hypoglycemic action of such EPS has been linked to the inhibition of α-glucosidase or α-amylase [60].

Decreasing postprandial hyperglycemia is the main priority for diabetes treatment. Academics have acknowledged that restricting glucosidase with inhibitors efficiently controls carbohydrate absorption and reduces the risk of postprandial hyperglycemia [61]. These inhibitors can potentially induce the liberation of glucagon-like peptide 1 (GLP-1) and subsequently elicit a decline in glycated hemoglobin [62]. EPSF8 extracted from *Pseudomonas* sp. strain AHG22 exhibited inhibitory potential against α-amylase and α-glucosidase. The results showed that EPSF8 had an IC_{50} of 93.1 $\mu g \cdot mL^{-1}$ for amylase inhibition (Figure 11), compared to that of 50.93 $\mu g \cdot mL^{-1}$ for the acarbose control (Figure S7). For α-glucosidase inhibition, EPSF8 had an IC_{50} of 127.28 $\mu g \cdot mL^{-1}$ (Figure 12) compared to that of 4.13 $\mu g \cdot mL^{-1}$ for the acarbose control (Figure S8). In line with our results, 11 *Annona muricata* endophytic bacterial strains inhibited α-amylase activity. With 72.22% inhibition, DS21, a G −ve bacterium, was the most active [63]. Bacteria's multifactorial inhibition of glucosidases remains undisclosed. It might be competitive or non-competitive inhibition, inhibitors bind to glucosidases' active sites, blocking substrate binding, non-competitive; the organism's metabolite binds to allosteric sites on glucosidases, modifying their conformation and blocking carbohydrate breakdown or substrate binding; bacteria-derived inhibitors bind to substrate, prevents where the substrate is bound. The mechanisms by which bacteria suppress different glucosidases may vary and require further *in vitro* and *in vivo* research [20].

Finally, EPSF8 was evaluated as a natural antimicrobial substitute and an alternative antibiofilm agent to antibiotics by agar well diffusion assay. A hole with a 6–8 mm diameter was punched aseptically with a sterile cork borer, and a volume (20–100 μL) of EPSF8 was supplemented on a Mueller–Hinton agar plate. After incubation, inhibition zones were represented as mm. The tested organisms were G +ve *B. subtilis* (ATCC 6633) *Staph. aureus* (ATCC 6538), and *E. faecalis* (ATCC 29212). G −ve bacteria were *E. coli* (ATCC 8739), *K. pneumoniae* (ATCC13883), and *S. typhi* (ATCC 6539). For the G +ve spectrum, the highest inhibition zone was found to be 46 ± 0.3 mm for *E. faecalis* (ATCC 29212), compared to that of 30 ± 0.4 mm for gentamicin. For the G −ve spectrum, the highest inhibition zone was 26 ± 0.2 mm for *S. typhi* (ATCC 6539) compared *to that of* 24 ± 0.3 mm gentamicin. EPSF8 exhibited antibacterial activity toward G +ve and G −ve ATCC bacteria (Figures 13–15).

In the MBC test, EPSF8 showed the lowest MBC of 7.8 $\mu g \cdot mL^{-1}$ against the G +ve bacterium *E. faecalis* (ATCC 29212). It had an MBC of 125 $\mu g \cdot mL^{-1}$ against the G −ve bacteria *K. pneumoniae* (ATCC 13883) and *S. typhi* (ATCC 6539) (Table 1). The MBC/MIC ratio indicated antibacterial activity. A ratio of MBC/MIC ≤4 indicates bactericidal impact, while a ratio >4 indicates bacteriostatic effect [64,65]. Based on the previous findings, we may conclude that EPSF8 has a bactericidal activity against both bacterial spectrums, especially for the G +ve bacterium *E. faecalis* (ATCC 29212) and against *E. coli* (ATCC 8739).

Next, the MTP plate assay was performed as an antibiofilm assay for the same bacterial spectrum (Figure 16), except for *E. coli*. Previous MICs and MBCs were used to test EPSF8 as an anti-biofilm. EPSF8 had the lowest antibiofilm activity (91.89%) for *Staph. aureus* at 75% MBC and the highest (93.47%) for *E. faecalis*. Concerning G −ve bacteria, EPSF8 had the lowest antibiofilm activity for *K. pneumoniae* (87.91%) and the highest for *S. typhi* (91.79 %) at 75% MBC.

In alignment with our research findings, an acidic EPSR3 extracted from *Bacillus cereus* from the Red Sea had an average molecular weight of 1.66×10^4 $g \cdot mol^{-1}$. It was found to have a strong inhibitory effect on *S. aureus* (MRSA). The study showed that a 5% concentration of EPSR3 for 60 min was enough to inhibit the growth of MRSA [7]. In contrast to our results, EPSF6 with a molecular weight of 2.7×10^4 $g \cdot mol^{-1}$ extracted from *B. velezensis* from the same source was examined for antimicrobial by MTP test against two pathogenic ATCC G +ve, two G −ve bacteria. However, neither significant activity was reported [9]. Microbial EPS acts against animal and plant bacteria alike. Drira *et al.* reported that EPS synthesized by *Porphyridium sordidum* could control fungal growth in

plants. EPS may serve as a stimulant to elevate the resilience of *A. thaliana* to *F. oxysporum*. [66].

EPSs exert antagonistic activity against pathogenic bacteria; for instance, in the context of *in vitro* experimentation; EPS synthesized by *Lactobacillus rhamnosus*, which was obtained from human breast milk, exhibited noteworthy antibacterial properties against the pathogenic bacteria *Salmonella enterica* serovar *Typhimurium* and *E. coli* [67]. The antimicrobial activity of EPS has also been found to correlate strongly with their physicochemical properties [68]. For example, negatively charged EPS derived from the *Lactococcus lactis* F-mou strain exhibited a more pronounced inhibitory effect on G +ve pathogens than G −ve ones. Notably, the strain *B. cereus* ATCC 10702 displayed the highest level of inhibition, indicating its susceptibility to the inhibitory action of the EPS [69]. As mentioned earlier, the findings postulated that the electrostatically charged EPS, specifically the sulfate groups, may facilitate enhanced interactions with G +ve bacteria. This can be attributed to the relatively higher positive charge exhibited by the cell walls of these bacteria.

Similarly, EPSF8 is a negatively charged hetero-EPS due to sulfate and uronic acid side chains, as clarified by FT-IR (Figure 2). Another disruptive impact of EPS is on the bacterial cell envelope, particularly the peptidoglycan layer, rendering it a plausible inhibitory mechanism [70]. This proposition was substantiated by the observation that EPSs such as kefiran exhibited interactions with bacterial or eukaryotic cells. Consequently, it was hypothesized that kefiran functioned as a masking or decoy agent, thereby exerting its inhibitory effects [71].

Therefore, it is likely that this particular action could impede the functionality of the receptors or channels located on the external membrane of the G −ve bacteria. While Zhou *et al.* suggested another mode of action, the presence of functional groups within the structure of EPS facilitates their interaction with bacterial cell envelopes, ultimately leading to antimicrobial activity [68], as in our explored EPSF8 (uronic acid = 14.70%, sulfate = 25.65% and *N*-acetyl glucosamine = 8.55%).

It is imperative to emphasize the limitations of embracing microbial EPS in industrial applications, particularly in the context of production and recovery processes. The elevated production costs primarily stem from utilizing costly and specialized nutrients in fermentation media formulation. This factor typically accounts for approximately 30% of the overall expenditure associated with the fermentation process. To optimize cost efficiency, it is advisable to employ more economical substrates, such as cane molasses, sugarcane bagasse, corn steep liquor, *etc.*, for large-scale production purposes [72].

Furthermore, the extraction methods for EPS can be appropriately adjusted to be economically viable and efficient. This modification would result in a substantial reduction in the overall expenses associated with subsequent processes. Finally, to attain elevated EPS yields, it is plausible to boost marine bacterial strains through genetic engineering techniques, such as mutagenic strains and gene manipulations [73]. Additionally, the production of EPS with distinct properties and structures can be accomplished by applying the same approaches [74].

5 Conclusions

EPSF8 is a hetero-acidic EPS sulfated and contains uronic acid and N-acetylglucosamine extracted from *Pseudomonas* sp. strain AHG22 isolated from the Red Sea, which could be considered as a green substitute for synthetic antioxidants aligning with its selective anti-cyclooxygenase properties. EPSF8 exhibited non-significant antidiabetic, less potent anti-inflammatory effects, and moderate hypocholesterolemic activity. However, it has proved to be considered a broad-spectrum, natural bactericidal, and antibiofilm compound of marine available origin, a potent substitute to traditional antibiotics. It is highly recommended that such findings be validated in different *in vivo* models and that their chemical structure and molecular formula be investigated. The findings above shed light on the prospective viability of *Pseudomonas* sp. strain AHG22 and its potential incorporation into the pharmaceutical industry.

Acknowledgments: The authors acknowledge the support *via* funding from Prince Sattam bin Abdulaziz University, Alkharj, Saudi Arabia, project number (PSAU/2024/R/1445).

Funding information: This study was supported *via* funding from Prince Sattam bin Abdulaziz University, Alkharj, Saudi Arabia, project number (PSAU/2024/R/1445).

Author contributions: Ghfren S. Aloraini: conceptualization, methodology, investigation, writing – original draft, writing – review and editing; Mona Othman I. Albureikan: methodology, validation, investigation, and writing – review and editing; Aisha M.A. Shahlol: methodology, validation, formal analysis, and writing – review and editing; Taghreed Shamrani: software, formal analysis, data curation, and visualization; Hussam Daghistani: software, formal analysis, data curation, visualization, and writing – review and editing; Mohammad El-Nablaway: methodology, formal analysis, and investigation; Nagwa A. Tharwat: conceptualization,

writing – review and editing, validation, writing – original draft, writing, and supervision; Ahmed M. Elazzazy: formal analysis, resources, visualization, data curation, and software; Ahmed F. Basyony: methodology, formal analysis, and writing – review and editing; Ahmed Ghareeb: conceptualization, methodology, investigation, writing – original draft, writing – review and editing and supervision. All authors have accepted responsibility for the entire content of this manuscript and approved its submission.

Conflict of interest: The authors state no conflict of interest.

Data availability statement: The data presented in this study are openly available in DDBJ/EMBL/Gen – Bank nucleotide sequence databases at https://www.ncbi.nlm.nih.gov/ (submitted on 06-MAY-2023), reference number GenBank: OQ931874.

References

[1] Barcelos, M. C.S., K. A.C. Vespermann, F. M. Pelissari, and G. Molina. Current status of biotechnological production and applications of microbial exopolysaccharides. *Critical Reviews in Food Science and Nutrition*, Vol. 60, 2020, pp. 1475–1495.

[2] Li, W., J. Ji, X. Chen, M. Jiang, X. Rui, and M. Dong. Structural elucidation and antioxidant activities of exopolysaccharides from Lactobacillus helveticus MB2-1. *Carbohydrate Polymers*, Vol. 102, 2014, pp. 351–359.

[3] Andrew, M. and G. Jayaraman. Structural features of microbial exopolysaccharides in relation to their antioxidant activity. *Carbohydrate Research*, Vol. 487, 2020, id. 107881.

[4] Xu, X., Y. Qiao, Q. Peng, B. Shi, and V. P. Dia. Antioxidant and immunomodulatory properties of partially purified exopolysaccharide from lactobacillus casei isolated from Chinese Northeast. Sauerkraut. *Immunological Investigations*, Vol. 51, 2022, pp. 748–765.

[5] Carocho, M., P. Morales, and I. C.F. R. Ferreira. Antioxidants: reviewing the chemistry, food applications, legislation and role as preservatives. *Trends in Food Science and Technology*, Vol. 71, 2018, pp. 107–120.

[6] Abdel-Wahab, B. A., H. F. Abd El-Kareem, A. Alzamami, C. A. Fahmy, B. H. Elesawy, M. Mostafa Mahmoud, et al. Novel exopolysaccharide from marine bacillus subtilis with broad potential biological activities: insights into antioxidant, anti-Inflammatory, cytotoxicity, and anti-alzheimer activity. *Metabolites*, Vol. 12, 2022, id. 715.

[7] Selim, S., M. S. Almuhayawi, M. T. Alharbi, M. K. Nagshabandi, A. Alanazi, M. Warrad, et al. In vitro assessment of antistaphylococci, antitumor, immunological and structural characterization of acidic bioactive exopolysaccharides from marine Bacillus cereus isolated from Saudi Arabia. *Metabolites*, Vol. 12, 2022, id. 132.

[8] Alshawwa, S. Z., K. S. Alshallash, A. Ghareeb, A. M. Elazzazy, M. Sharaf, A. Alharthi, et al. Assessment of pharmacological potential of novel exopolysaccharide isolated from marine Kocuria sp. Strain AG5: broad-spectrum biological investigations. *Life*, Vol. 12, 2022, id. 1387.

[9] Alharbi, M. A., A. A. Alrehaili, M. O.I. Albureikan, A. F. Gharib, H. Daghistani, M. M. Bakhuraysah, et al. In vitro studies on the pharmacological potential, anti-tumor, antimicrobial, and acetylcholinesterase inhibitory activity of marine-derived Bacillus velezensis AG6 exopolysaccharide. *RSC Advances*, Vol. 13, 2023, pp. 26406–26417.

[10] Alharbi, N. K., Z. F. Azeez, H. M. Alhussain, A. M. A. Shahlol, M. O. I. Albureikan, M. G. Elsehrawy, et al. Tapping the biosynthetic potential of marine *Bacillus licheniformis* LHG166, a prolific sulphated exopolysaccharide producer: structural insights, bioprospecting its antioxidant, antifungal, antibacterial and anti-biofilm potency as a novel anti-infective lead. *Front Microbiol*. Vol. 15, 2024, id. 1385493.

[11] Chaisuwan, W., Y. Phimolsiripol, T. Chaiyaso, C. Techapun, N. Leksawasdi, K. Jantanasakulwong, et al. The antiviral activity of bacterial, fungal, and algal polysaccharides as bioactive ingredients: potential uses for enhancing immune systems and preventing viruses. *Frontiers in Nutrition*, Vol. 8, 2021, id. 902.

[12] Wang, Q., M. Wei, J. Zhang, Y. Yue, N. Wu, L. Geng, et al. Structural characteristics and immune-enhancing activity of an extracellular polysaccharide produced by marine Halomonas sp. 2E1. *International Journal of Biological Macromolecules*, Vol. 183, 2021, pp. 1660–1668.

[13] Chatterjee, S., S. Mukhopadhyay, S. S. Gauri, and S. Dey. Sphingobactan, a new α-mannan exopolysaccharide from Arctic Sphingobacterium sp. IITKGP-BTPF3 capable of biological response modification. *International Immunopharmacology*, Vol. 60, 2018, pp. 84–95.

[14] Abdalla, A. K., M. M. Ayyash, A. N. Olaimat, T. M. Osaili, A. A. Al-Nabulsi, N. P. Shah, et al. Exopolysaccharides as antimicrobial agents: mechanism and spectrum of activity. *Frontiers in Microbiology*, Vol. 12, 2021, id. 664395.

[15] Bello-Morales, R., S. Andreu, V. Ruiz-Carpio, I. Ripa, and J. A. López-Guerrero. Extracellular polymeric substances: still promising antivirals. *Viruses*, Vol. 14, 2022, id. 1337.

[16] Rubini, D., P. V. Varthan, S. Jayasankari, B. N. Vedahari, and P. Nithyanand. Suppressing the phenotypic virulence factors of Uropathogenic Escherichia coli using marine polysaccharide. *Microbial Pathogenesis*, Vol. 141, 2020, id. 103973.

[17] Wu, S., G. Liu, W. Jin, P. Xiu, and C. Sun. Antibiofilm and anti-infection of a marine bacterial exopolysaccharide against *pseudomonas aeruginosa*. *Frontiers in Microbiology*, Vol. 7, 2016, (accessed January 29, 2023).

[18] Khodeer, D.M., A. M. Nasr, A. M. Swidan, S. Shabayek, R. M. Khinkar, M. M. Aldurdunji, et al. Characterization, antibacterial, antioxidant, antidiabetic, and anti-inflammatory activities of green synthesized silver nanoparticles using Phragmanthera austroarabica A. G. Mill and J. A. Nyberg extract. *Front. Microbiol*, Vol. 13, 2023, id. 1078061.

[19] Singla, P., A. Bardoloi, and A. A. Parkash. Metabolic effects of obesity: A review. *World Journal of Diabetes*, Vol. 1, 2010, pp. 76–88.

[20] Wang, X., J. Li, J. Shang, J. Bai, K. Wu, J. Liu, et al. Metabolites extracted from microorganisms as potential inhibitors of glycosidases (α-glucosidase and α-amylase): A review. *Frontiers in Microbiology*, Vol. 13, 2022, id. 1050869.

[21] Zeng, Z., S.-Y. Huang, and T. Sun. Pharmacogenomic studies of current antidiabetic agents and potential new drug targets for precision medicine of diabetes. *Diabetes Therapy*, Vol. 11, 2020, pp. 2521–2538.

[22] Hayakawa, M. And H. Nonomura. Humic acid-vitamin agar, a new medium for the selective isolation of soil actinomycetes. *Journal of Fermentation Technology*, Vol. 65, 1987, pp. 501–509.

[23] Krieg, N. R., J. T. Staley, D. R. Brown, B. P. Hedlund, B. J. Paster, N. L. Ward, et al., (Eds.) *Bergey's Manual® of Systematic Bacteriology*, Springer, New York, New York, NY, 2010.
[24] Tamura, K., D. Peterson, N. Peterson, G. Stecher, M. Nei, and S. Kumar. MEGA5: Molecular evolutionary genetics analysis using maximum likelihood, evolutionary distance, and maximum parsimony methods. *Molecular Biology and Evolution*, Vol. 28, 2011, pp. 2731–2739.
[25] Liu, C., J. Lu, L. Lu, Y. Liu, F. Wang, and M. Xiao. Isolation, structural characterization and immunological activity of an exopolysaccharide produced by Bacillus licheniformis 8-37-0-1. *Bioresource Technology*, Vol. 101, 2010, pp. 5528–5533.
[26] Wang, H., X. Jiang, H. Mu, X. Liang, and H. Guan. Structure and protective effect of exopolysaccharide from P. Agglomerans strain KFS-9 against UV radiation. *Microbiological Research*, Vol. 162, 2007, pp. 124–129.
[27] Nicely, W. B. Infrared spectra of carbohydrates. In: *Advances in carbohydrate chemistry*, M. L. Wolfrom, Tipson, R. S., (Eds.), Academic Press, 1957, pp. 13–33.
[28] Filisetti-Cozzi, T. M. and N. C. Carpita. Measurement of uronic acids without interference from neutral sugars. *Analytical Biochemistry*, Vol. 197, 1991, pp. 157–162.
[29] Garrido, M. L. Determination of sulphur in plant material. *Analyst*, Vol. 89, 1964, pp. 61–66.
[30] Randall, R. C., G. O. Phillips, P. A. Williams. The role of the proteinaceous component on the emulsifying properties of gum arabic. *Food Hydrocolloids*, Vol. 2, No. 2, 1988, pp. 131–140.
[31] Brand-Williams, W., M. E. Cuvelier, and C. Berset. Use of a free radical method to evaluate antioxidant activity. *LWT – Food Science and Technology*, Vol. 28, 1995, pp. 25–30.
[32] Ruch, R. J., K. A. Crist, and J. E. Klaunig. Effects of culture duration on hydrogen peroxide-induced hepatocyte toxicity. *Toxicology and Applied Pharmacology*, Vol. 100, 1989, pp. 451–464.
[33] Miller, N. J. and C. A. Rice-Evans. The relative contributions of ascorbic acid and phenolic antioxidants to the total antioxidant activity of orange and apple fruit juices and blackcurrant drink. *Food Chemistry*, Vol. 60, 1997, pp. 331–337.
[34] Balakrishnan, N., A. B. Panda, N. R. Raj, A. Shrivastava, and R. Prathani. The evaluation of nitric oxide scavenging activity of acalypha indica linn root. *Asian Journal of Research in Chemistry*, Vol. 2, 2009, pp. 148–150.
[35] Prieto, P., M. Pineda, and M. Aguilar. Spectrophotometric quantitation of antioxidant capacity through the formation of a phosphomolybdenum complex: specific application to the determination of vitamin E. *Analytical Biochemistry*, Vol. 269, 1999, pp. 337–341.
[36] Lahmass, I., S. Ouahhoud, M. Elmansuri, A. Sabouni, E. Mohammed, R. Benabbas, et al. Determination of antioxidant properties of six by-products of crocus sativus l. (saffron) plant products. *Waste and Biomass Valorization*, Vol. 9, 2018, pp. 1349–1357.
[37] Benzie, I. F. and J. J. Strain. The ferric reducing ability of plasma (FRAP) as a measure of "antioxidant power": the FRAP assay. *Analytical Biochemistry*, Vol. 239, 1996, pp. 70–76.
[38] Athamena, S., S. Laroui, W. Bouzid, and A. Meziti. The antioxidant, anti-inflammatory, analgesic and antipyretic activities of Juniperu thurifera. *Journal of Herbs, Spices and Medicinal Plants*, Vol. 25, 2019, pp. 271–286.
[39] Granica, S., M. E. Czerwińska, J. P. Piwowarski, M. Ziaja, and A. K. Kiss. Chemical composition, antioxidative and anti-Inflammatory activity of extracts prepared from aerial parts of Oenothera biennis L. And Oenothera paradoxa Hudziok obtained after seeds cultivation. *Journal of Agricultural and Food Chemistry*, Vol. 61, 2013, pp. 801–810.
[40] Amessis-Ouchemoukh, N., K. Madani, P. L.V. Falé, M. L. Serralheiro, and M. E.M. Araújo. Antioxidant capacity and phenolic contents of some Mediterranean medicinal plants and their potential role in the inhibition of cyclooxygenase-1 and acetylcholinesterase activities. *Industrial Crops and Products*, Vol. 53, 2014, pp. 6–15.
[41] Gorun, V., I. Proinov, V. Băltescu, G. Balaban, and O. Bârzu. Modified Ellman procedure for assay of cholinesterases in crude enzymatic preparations. *Analytical Biochemistry*, Vol. 86, 1978, pp. 324–326.
[42] Roh, C., and U. Jung, Screening of crude plant extracts with anti-obesity activity, *International Journal of Molecular Sciences*, Vol. 13, 2012, pp. 1710–1719.
[43] Wickramaratne, M. N., J. C. Punchihewa, and D. B.M. Wickramaratne. In-vitro alpha amylase inhibitory activity of the leaf extracts of Adenanthera pavonina. *BMC Complementary and Alternative Medicine*, Vol. 16, 2016, p. 466.
[44] Pistia-Brueggeman, G. and R. I. Hollingsworth. A preparation and screening strategy for glycosidase inhibitors. *Tetrahedron*, Vol. 57, 2001, pp. 8773–8778.
[45] Magaldi, S., S. Mata-Essayag, C. Hartung de Capriles, C. Perez, M. T. Colella, C. Olaizola, et al. Well diffusion for antifungal susceptibility testing. *International Journal of Infectious Diseases*, Vol. 8, 2004, pp. 39–45.
[46] Brown, W. J. National committee for clinical laboratory standards agar dilution susceptibility testing of anaerobic gram-negative bacteria. *Antimicrobial Agents and Chemotherapy*, Vol. 32, 1988, pp. 385–390.
[47] Antunes, A. L.S., D. S. Trentin, J. W. Bonfanti, C. C.F. Pinto, L. R.R. Perez, A. J. Macedo, et al. Application of a feasible method for determination of biofilm antimicrobial susceptibility in staphylococci. *APMIS*, Vol. 118, 2010, pp. 873–877.
[48] Min, W.-H., X.-B. Fang, T. Wu, L. Fang, C.-L. Liu, J. Wang, Characterization and antioxidant activity of an acidic exopolysaccharide from Lactobacillus plantarum JLAU103. *Journal of Bioscience and Bioengineering*, Vol. 127, 2019, pp. 758–766.
[49] Giménez-Bastida, J. A., T. Shibata, K. Uchida, and C. Schneider. Roles of 5-lipoxygenase and cyclooxygenase-2 in the biosynthesis of hemiketals E2 and D2 by activated human leukocytes. *FASEB Journal*, Vol. 31, 2017, pp. 1867–1878.
[50] Attiq, A., J. Jalil, K. Husain, and W. Ahmad. Raging the war against inflammation with natural products. *Frontiers in Pharmacology*, Vol. 9, 2018, id. 976.
[51] Jenab, A., R. Roghanian, and G. Emtiazi. Bacterial natural compounds with anti-inflammatory and immunomodulatory properties (Mini Review). *Drug design, Development and Therapy*, Vol. 14, 2020, pp. 3787–3801.
[52] Čolović, M. B., D. Z. Krstić, T. D. Lazarević-Pašti, A. M. Bondžić, and V. M. Vasić. Acetylcholinesterase Inhibitors: Pharmacology and Toxicology. *Current Neuropharmacology*, Vol. 11, 2013, pp. 315–335.
[53] Nordberg, A., C. Ballard, R. Bullock, T. Darreh-Shori, and M. Somogyi. A review of butyrylcholinesterase as a therapeutic target in the treatment of alzheimer's diseaseprim. *The primary care companion for CNS disorders*, Vol. 15, No. 2, 2013, id. 12r01412.
[54] Almasi, F., F. Mohammadipanah, H.-R. Adhami, and J. Hamedi. Introduction of marine-derived Streptomyces sp. UTMC 1334 as a

source of pyrrole derivatives with anti-acetylcholinesterase activity. *Journal of Applied Microbiology*, Vol. 125, 2018, pp. 1370–1382.

[55] Gangalla, R., S. Gattu, S. Palaniappan, M. Ahamed, B. Macha, R. K. Thampu, et al. Structural characterisation and assessment of the novel Bacillus *amyloliquefaciens* rk3 exopolysaccharide on the improvement of cognitive function in alzheimer's disease mice. *Polymers*, Vol. 13, 2021, id. 2842.

[56] Pasinetti, G. M. Cyclooxygenase and inflammation in Alzheimer's disease: experimental approaches and clinical interventions. *Journal of Neuroscience Research*, Vol. 54, 1998, pp. 1–6.

[57] Dilna, S. V., H. Surya, R. G. Aswathy, K. K. Varsha, D. N. Sakthikumar, A. Pandey, et al. Characterization of an exopolysaccharide with potential health-benefit properties from a probiotic Lactobacillus plantarum RJF4. *LWT-Food Science and Technology*, Vol. 64, 2015, pp. 1179–1186.

[58] Sasikumar, K., D. Kozhummal Vaikkath, L. Devendra, and K. M. Nampoothiri. An exopolysaccharide (EPS) from a Lactobacillus plantarum BR2 with potential benefits for making functional foods. *Bioresource Technology*, Vol. 241, 2017, pp. 1152–1156.

[59] Korcz, E. and L. Varga. Exopolysaccharides from lactic acid bacteria: Techno-functional application in the food industry. *Trends in Food Science and Technology*, Vol. 110, 2021, pp. 375–384.

[60] Al-Dhaheri, A. S., R. Al-Hemeiri, J. Kizhakkayil, A. Al-Nabulsi, A. Abushelaibi, N. P. Shah, et al. Health-promoting benefits of low-fat akawi cheese made by exopolysaccharide-producing probiotic Lactobacillus plantarum isolated from camel milk. *Journal of Dairy Science*, Vol. 100, 2017, pp. 7771–7779.

[61] Asano, N. Glycosidase inhibitors: update and perspectives on practical use. *Glycobiology*, Vol. 13, 2003, pp. 93R–104R.

[62] Kumar, R. V. and V. R. Sinha. Newer insights into the drug delivery approaches of α-glucosidase inhibitors. *Expert Opinion on Drug Delivery*, Vol. 9, 2012, pp. 403–416.

[63] Pujiyanto, S., M. Resdiani, B. Raharja, and R. S. Ferniah. A-Amylase inhibitor activity of endophytic bacteria isolated from Annona muricata L. *Journal of Physics: Conference Series*, Vol. 1025, 2018, id. 012085.

[64] Levison, M. E. Pharmacodynamics of antimicrobial drugs. *Infectious Disease Clinics of North America*, Vol. 18, 2004, pp. 451–465.

[65] Thomas, B., A. Adeleke, R. Raheem-Ademola, R. Kolawole, and O. Musa. Efficiency of some disinfectants on bacterial wound pathogens. *Life Science Journal*, Vol. 9, 2012, pp. 752–755.

[66] Drira, M., J. Elleuch, H. Ben Hlima, F. Hentati, C. Gardarin, C. Rihouey, et al. Optimization of exopolysaccharides production by porphyridium sordidum and their potential to induce defense responses in arabidopsis thaliana against *Fusarium oxysporum*. *Biomolecules*, Vol. 11, 2021, id. 282.

[67] Rajoka, M. S.R., H. M. Mehwish, H. F. Hayat, N. Hussain, S. Sarwar, H. Aslam, et al. Characterization, the antioxidant and antimicrobial activity of exopolysaccharide isolated from poultry origin lactobacilli. *Probiotics and Antimicrobial Proteins*, Vol. 11, 2019, pp. 1132–1142.

[68] Zhou, Y., Y. Cui, and X. Qu. Exopolysaccharides of lactic acid bacteria: Structure, bioactivity and associations: A review. *Carbohydrate Polymers*, Vol. 207, 2019, pp. 317–332.

[69] Nehal, F., M. Sahnoun, S. Smaoui, B. Jaouadi, S. Bejar, and S. Mohammed. Characterization, high production and antimicrobial activity of exopolysaccharides from Lactococcus lactis F-mou. *Microbial Pathogenesis*, Vol. 132, 2019, pp. 10–19.

[70] Sivasankar, P., P. Seedevi, S. Poongodi, M. Sivakumar, T. Murugan, L. Sivakumar, et al. Characterization, antimicrobial and antioxidant property of exopolysaccharide mediated silver nanoparticles synthesized by Streptomyces violaceus MM72. *Carbohydrate Polymers*, Vol. 181, 2018, pp. 752–759.

[71] Medrano, M., M. F. Hamet, A. G. Abraham, and P. F. Pérez. Kefiran protects Caco-2 cells from cytopathic effects induced by Bacillus cereus infection. *Antonie Van Leeuwenhoek*, Vol. 96, 2009, pp. 505–513.

[72] Dave, S. R., K. H. Upadhyay, A. M. Vaishnav, and D. R. Tipre. Exopolysaccharides from marine bacteria: production, recovery and applications. *Environmental Sustainability*, Vol. 3, 2020, pp. 139–154.

[73] Yang, M., J. Yun, H. Zhang, T. A. Magocha, H. Zabed, Y. Xue, et al. Genetically engineered strains: application and advances for 1,3-propanediol production from glycerol. *Food Technology and Biotechnology*, Vol. 56, 2018, pp. 3–15.

[74] Levander, F., M. Svensson, and P. Rådström. Enhanced exopolysaccharide production by metabolic engineering of *Streptococcus thermophilus*. *Applied and Environmental Microbiology*, Vol. 68, 2002, pp. 784–790.